

1 (2007

LIBRARY Michigan State University

This is to certify that the

thesis entitled

Functionalization of Mesoporous Molecular Sieves Assembled Using Non-Ionic Surfactants and Water Soluble Silicates; Synthesis and Characterization

presented by

Jainisha R Shah

has been accepted towards fulfillment of the requirements for

M.S. degree in Chemistry

Major professo

Date December 11, 2001

MSU is an Affirmative Action/Equal Opportunity Institution

O-7639

PLACE IN RETURN BOX to remove this checkout from your record. **TO AVOID FINES** return on or before date due. **MAY BE RECALLED** with earlier due date if requested.

DATE DUE	DATE DUE	DATE DUE

2/05 p:/CIRC/DateDue.indd-p.1

FUNCTIONALIZATION OF MESOPOROUS MOLECULAR SIEVES ASSEMBLED USING NON-IONIC SURFACTANTS AND WATER SOLUBLE SILICATES; SYNTHESIS AND CHARACTERIZATION

By

Jainisha R. Shah

A THESIS

Submitted to
Michigan State University
In partial fulfillment of the requirements
For the degree of

MASTER OF SCIENCE

Department of Chemistry

2001

ABSTRACT

FUNCTIONALIZATION OF MESOPOROUS MOLECULAR SIEVES ASSEMBLED USING NON-IONIC SURFACTANTS AND WATER SOLUBLE SILICATES: SYNTHESIS AND CHARACTERIZATION

By

Jainisha R. Shah

The organofunctionalization of mesostructured silicas is an important current area of research because of the potential applications of these materials as catalytic and trapping agents. Current assembly techniques utilize siloxane precursors as starting materials that limit the potential applications due to the high cost of the reagents and processing methods. The synthesis of stable mesostructured silica denoted MSU-X' has been accomplished in our group using cost effective starting materials viz. water soluble sodium silicate and non-ionic surfactants. Presented here is the synthesis and characterization of organofunctionalized MSU-X' mesostructures in a one step assembly procedure using 3-Mercaptopropyltrimethoxysilane as the organosilane reagent and sodium silicate as the framework precursor and PEO surfactant as the structure directors. The characterization of these materials was done by powder X-ray diffraction, N₂ adsorption-desorption isotherms, Transmission electron microscopy, and ²⁹Si NMR spectroscopy. This is the first reported direct synthesis of organofunctionalized mesostructured silica based on sodium silicate as a reagent. A model for the assembly of these mesostructure materials is presented.

Dedicated to my parents

ACKNOWLEDGEMENTS

I would like to take this opportunity to thank Dr. Pinnavaia for his guidance and his support. I am grateful for his patience and all the encouragement he provided in the last couple of years. I am especially appreciative of him for believing in me.

I would also like to thank all the Pinnavaia group members present and current for their support and friendship and for all the helpful discussions. I would like to specially thank Dr. Seong-Su Kim for his patience and helpful ideas and discussions throughout the two years.

Lastly I would like to thank my family and friends for motivating me to come here for graduate school. I am especially thankful to my parents, as without their support none of this would be possible.

TABLE OF CONTENTS

LIS	ST OF	TABLESvii
LIS	ST OF	FIGURESviii
ΑB	BREV	/IATIONSx
1.	Chap	ter 1 : Introduction1
	1.1 [Definitions of Porous Solids2
	1.2 \$	Synthesis of Mesoporous Molecular Sieves2
	-	1.2.1. Electrostatic (S ⁺ I ⁻) Assembly of Mesoporous Molecular
		Sieves2
	1	.2.2. Additional Electrostatic Pathways7
	1	.2.3. Neutral (S ⁰ I ⁰) Assembly to Mesoporous Molecular Sieves7
	1	.2.4 Non-ionic Assembly Pathways to Mesoporous Molecular
		Sieves7
	1.3	Advances in Mesoporous Molecular Sieves8
	•	I.3.1 Low pH Conditions with PEO Based Surfactants8
	-	1.3.2 Synthesis of Stable Mesostructured Silicas from PEO
		Based Surfactants and Water Soluble Silica Sources9
	1.4	Functionalization10
	1.5	Research Objectives16
	1.6	References17
2	Chap	oter 2 Synthesis of Mesoporous Silicas from Non-ionic
		Surfactants And Water Soluble Silicas23
	2.1	Introduction23
	2.2	Experimental25
		2.2.1 Synthesis of MP-MSU-X' from Tween 80 and Brij 56
		Surfactants and Sodium Silicate26
		2.2.2 Physical Measurements
	2.3	Results and Discussion
		2.3.1 Mesostructures Assembled Using Tween 80

		Surfactant	27
		2.3.2 Mesostructures Assembled Using Brij 56	6
		Surfactant	37
	2.4	Conclusions	49
	2.5	References	55
3	Chap	oter 3 Future Goals	
	3.1	Functionalization of MSU-X' mesostructures with	h
		other organosilanes	57
	3.2	Functionalization of large pore foam like MSU-F	:
		mesostructures	58
	3.3	Functionalization of MSU-SA Mesostructures	60
	3.4	References	61

LIST OF TABLES

Table 2.1	Physical properties of MP-MSU-X' mesostructures	
	assembled using Tween 80 surfactant	33
Table 2.2	²⁹ Si MAS NMR Cross-linking parameters for MP-	
	MSU-X' mesostructures assembled using Tween 80	
	surfactant	35
Table 2.3	X-ray diffraction values for MP-MSU-X'	
	mesostructures assembled using Brij 56 surfactant	39
Table 2.4	Physical properties of MP-MSU-X' mesostructures	
	assembled using Brij 56 surfactant	47
Table 2.5	²⁹ Si MAS NMR Cross-linking parameters for MP-	
	MSU-X'mesostructures assembled using Brij 56	
	surfactant4	48
Table 2.6	Comparison of MP-MSU-X and MP-MSU-X'	
	mesostructured materials assembled using various	
	non- ionic surfactants	53

LIST OF FIGURES

Figure 1.1	Mechanism of silicate induced ordering of hexagonally	•
	ordered surfactant-silicate structure. Calcination resulting	
	in MCM-41 silica with accessible pore volume	3
Figure 1.2	Powder X-ray diffraction pattern of calcined hexagonal	
	MCM-41	5
Figure 1.3	N ₂ adsorption-desorption isotherm of calcined MCM-41	6
Figure 1.4	Schematic representation for the grafting of organosilane	
	on mesoporous molecular sieve	13
Figure 1.5	Schematic representation of mesoporous molecular sieve	
	functionalized by direct synthesis	15
Figure 2.1	Powder X-ray diffraction patterns for MP functionalized	
	MP-MSU-X' silicas assembled using Tween 80	
	surfactant	29
Figure 2.2	N ₂ adsorption-desorption isotherm for MP functionalized	
	MSU-X' silicas from x MP and (1-x) sodium silicate	
	mixtures in the presence of Tween 80 as the	
	surfactant	30
Figure 2.3	Horvath-Kawazoe pore size distributions obtained from the	
	N ₂ adsorption-desorption isotherms of the MP-MSU-X'	
	mesostructures described in Figure 2.2	31
Figure 2.4	²⁹ Si MAS NMR spectra of MP-MSU-X' assembled using	
	Tween 80 surfactant	35
Figure 2.5	TEM images of (a) MSU-X' and (b) 20% MP-MSU-X'	
	assembled using Brij 56 as the surfactant	36
Figure 2.6	Powder X-ray diffraction patterns for MP functionalized	
	MP-MSU-X' silicas assembled using Brij 56 surfactant	39
Figure 2.7	• •	
~	MSU-X' and (c, d) 15% MP-MSU-X' assembled using Brij	

	56 surfactant	40
Figure 2.8	Scheme 1: Diagram of interaction of PEO surfactant, silica	
	and metal cations and induction of gauche conformation	
	by M ⁺ cations	41
Figure 2.9	Scheme 2: Diagram of interaction between M ⁺ cations	
	linking PEO surfactant headgroups	42
Figure 2.10	N ₂ adsorption-desorption isotherm for MP functionalized	
	MSU-X' silicas from x MP and (1-x) sodium silicate	
	mixtures in the presence of Brij 56 as the surfactant	45
Figure 2.11	Horvath-Kawazoe pore size distributions obtained from the	
	N_2 adsorption-desorption isotherms of the MP-MSU-X $^\prime$	
	mesostructures described in Figure 2.8	46
Figure 2.12	²⁹ Si MAS NMR spectra of MP-MSU-X' assembled using	
	Brij 56 surfactant	48
Figure 2.13	Schematic representation of the steps involved in the	
	assembly of MP-MSU-X' mesostructures from 3-	
	mercaptopropyltrimethoxysilane (3-MPTMS) and sodium	
	silicate in the presence of Brij 56 surfactant. The electrical	
	charge on the silicate anion and the bonding of Na ⁺ to the	
	PEO head groups are not shown for clarity	52

LIST OF ABBREVIATIONS

BET Brunauer-Emmett-Teller

BJH Barrett-Joyner-Halenda

EtOH Ethanol

H-bonding Hydrogen bonding

HK Horvath and Kawazoe pore size distribution model

HMS Hexagonal Mesoporous Silica

1 Anionic inorganic precursor

I⁺ Cationic inorganic precursor

I⁰ Neutral inorganic precursor

IUPAC International Union of Pure and Applied Chemistry

M⁺ Metal cation

MAS Magic Angle Spinning

MCM-41 Mobil Composition of Matter 41

MCF Mesostructured Cellular Foam

mmol Millimoles

3-MPTMS 3-Mercaptopropyltrimethoxysilane

MSU-F Large pore mesostructured silicas synthesized with P123

surfactant, trimethylbenzene and water soluble silicates at

near neutral assembly conditions

MSU-H Hexagonal mesostructured silicas synthesized using PEO

based surfactants and water soluble silicates at near neutral

assembly conditions

MSU-SA Mesostructured silicas synthesized with amine surfactant and

water soluble silicates

MSU-X Wormhole mesostructured silicas synthesized with PEO

based surfactants and TEOS under neutral (N°I°) assembly

conditions

MSU-X' Wormhole mesostructured silicas synthesized with PEO

based surfactants and water soluble silicates under neutral

(N⁰I^O) assembly conditions

MP-MSU-X' Mercaptopropyl functionalized MSU-X' mesostructured

silicas

MP-MSU-F Mercaptopropyl functionalized MSU-F mesostructured silicas

nm Nanometer (10⁻⁹ m)

NMR Nuclear Magnetic Resonance

N⁰ Non-ionic amphiphilic PEO based surfactant

N°I° Neutral assembly pathway utilizing H-bonding between PEO

based surfactant and inorganic precursor

P/Po Relative pressure P = Pressure Po = Saturation pressure

PEO Polyethylene oxide

ppm Parts per million

PXRD Powder X-ray diffraction

Q² Incompletely condensed silica sites Si(OSi)₂(OH)₂

Q³ Incompletely condensed silica sites Si(OSi)₃(OH)

Q⁴ Completely condensed silica sites Si(OSi)₄

S Anionic amphiphilic surfactant

S⁺ Cationic amphiphilic surfactant

S⁺I⁻ Pathway 1 electrostatic assembly between cationic surfactant

and anionic silica precursor

S⁺X⁻I⁺ Electrostatic assembly between cationic surfactant and

cationic silica precursors halogen ions as mediating counter

ions

SBA Mesostructured silicas assembled under high acid low pH

conditions with TEOS as the inorganic precursor

SBA-15 Large pore hexagonal mesostructured silica assembled

under high acid low pH conditions with TEOS as the

inorganic precursor and triblock copolymer PEO based

surfactant

S_{BET} Specific surface area in m²/g obtained from the linear part of

the adsorption isotherm using Brunauer Emmett Teller

equation

S⁰ Neutral amphiphilic amine surfactant

S⁰I⁰ Neutral assembly pathway between neutral amine surfactant

and TEOS

TEOS Tetraethylorthosilicate

T² Functionalized Q² site RSi(OSi)₃OH

T³ Functionalized Q³ site RSi(OSi)₃

TMB Trimethylbenzene

X Halogen or anionic counter ion

Chapter 1

Introduction

1.1 Definitions of Porous solids:

Porous materials have vast number of practical applications in various areas. They are used as adsorbents, ion exchangers, catalysts, sensory materials, and heavy metal ion traps¹⁻⁴. Though porous materials have various compositions all of them contain accessible void space, defined as framework porosity within their interior structure. The aggregation or intergrowth of small grains in solid particle results in the formation of pores between these grains and these pores are defined as intra particle or textural porosity.

Porous materials are classified by IUPAC as⁵

- (a) Microporous materials with pores < 2 nm in diameter
- (b) Macroporous materials with pores > 50 nm in diameter
- (c) Mesoporous materials, which are intermediate in the range between 2-50 nm.

One of the classes of porous materials is zeolite. They have uniform pore size and hence are good candidates for many of the applications such as catalysis, adsorption, separation and ion exchange. Zeolites have also been used to remove water from gases⁶, separate glucose from fructose⁷, and to soften water in detergents⁸. The most important application of the zeolites would be their use as catalysts in fluid catalytic cracking of petroleum fractions⁹. However, one disadvantage is that the zeolites have small pore size (~0.74 nm), which prevents the large hydrocarbon molecules from penetrating the pore

volume and being converted to gasoline. In this case, as in many, others, small pore size limits the usefulness of zeolites.

1.2 Synthesis of Mesoporous Molecular Sieves

1.2.1 Electrostatic S[†]I⁻ Assembly of Mesoporous Molecular

Sieves Silica

Once scientists recognized the drawbacks of zeolites, they attempted to increase the pore size of these molecular sieves. A breakthrough in this field came about in 1992 when researchers from Mobil synthesized mesoporous silicate using organic cation surfactant assemblies. Mobil researchers were able to assemble mesoporous molecular sieves from aluminosilicates and purely siliceous gels with pore sizes in the range of 2-10 nm and uniform pore size distributions 10,11. The surfactants are used as templates and have a long hydrophobic alkyl chain and hydrophilic quaternary ammonium cations. When dissolved in aqueous solutions these surfactants spontaneously orient themselves to form surfactant assemblies or micelles. Long chain amphiphillic quaternary ammonium surfactants of the type [C_nH_{2n+1}(CH₃) ₃N]⁺ minimize their energy in solution by forming micelles, in these micelles the hydrophobic alkyl chain arranged in the interior and the charged head group at the exterior of the micelle^{10,11}. These surfactants can form different mesophases in solution depending on certain factors such as concentration. One such phase consists of cylindrical rod like surfactant micelles. Addition of a basic silica species such as sodium silicate to the surfactant solution and subsequent synthesis under hydrothermal conditions resulted in the formation of cationic surfactant (S⁺) micelle and anionic silica species $(\Gamma)^{10}$. The resulting pore structure formed through the electrostatic $(S^*\Gamma)$ pathway illustrated in Figure $(1.1)^{12}$ mimics the formation of liquid crystal phases known for these surfactants. Mobil researchers were able to tailor mesopore size of the molecular sieves by (a) varying surfactant chain length $(C_n)^{10}$ (b) addition of auxiliary agents or (c) post synthetic treatment to reduce the pore size 10 .

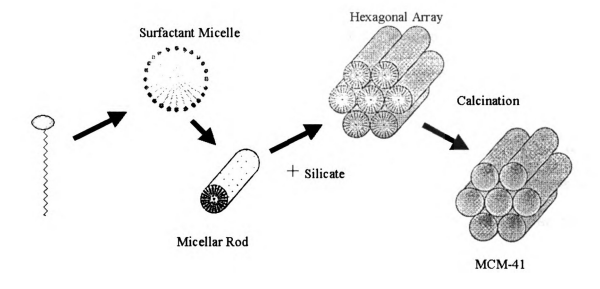


Fig 1.1 Mechanism of silicate induced ordering of hexagonally ordered surfactant-silicate structures. Calcination resulting in MCM-41silica with accessible pore volume.

The composition of a typical reaction mixture for the preparation of the MCM-41 is as follows

1.0 SiO₂: 0.03 Al₂O₃: 0.007 Na₂O: 0.183 (CTMA) _{2O}: 0.156 (TMA) _{2O}: 23.5 H₂O

The preparation consists of mixing these inorganic precursors with the surfactant solution and autoclaving the mixture at $100-150^{\circ}$ C for 4-144 hours. The product was then recovered by filtration, washed with water and air-dried. The surfactant was removed by calcination at 550° C for 1hr in flowing N_2 and 6 hours in air at the same temperature.

The mesophases formed are characterized by powder X-ray diffraction. Powder X-ray diffraction patterns of MCM-41 (Figure 1.2) characteristically show at least 3 peaks (d_{100} , d_{110} , d_{200}) that can be indexed to the hexagonal unit cell with a unit cell parameter $a_0 = 2d_{100}/\sqrt{3}$.

Adsorption studies of these materials show isotherms (Figure 1.3) with a sharp step characteristic of adsorption uptake due to capillary condensation within the framework mesopores. The relative pressure at which the step occurs is determined by the pore and shifts to higher relative pressures as the pore diameter increases. BET surface areas are estimated to be approximately 1000 m²/g. Mesopore volumes range from 0.7-1.2 cm³/g. Pore size distribution is calculated from the adsorption branch with the Horvath Kawazoe model¹³.

The mechanism for the assembly of long range ordered MCM-41 was explained as the electrostatic charge matching assembly (S^+I^-) between the cationic surfactant (S^+) and anionic inorganic precursor (I^-) .

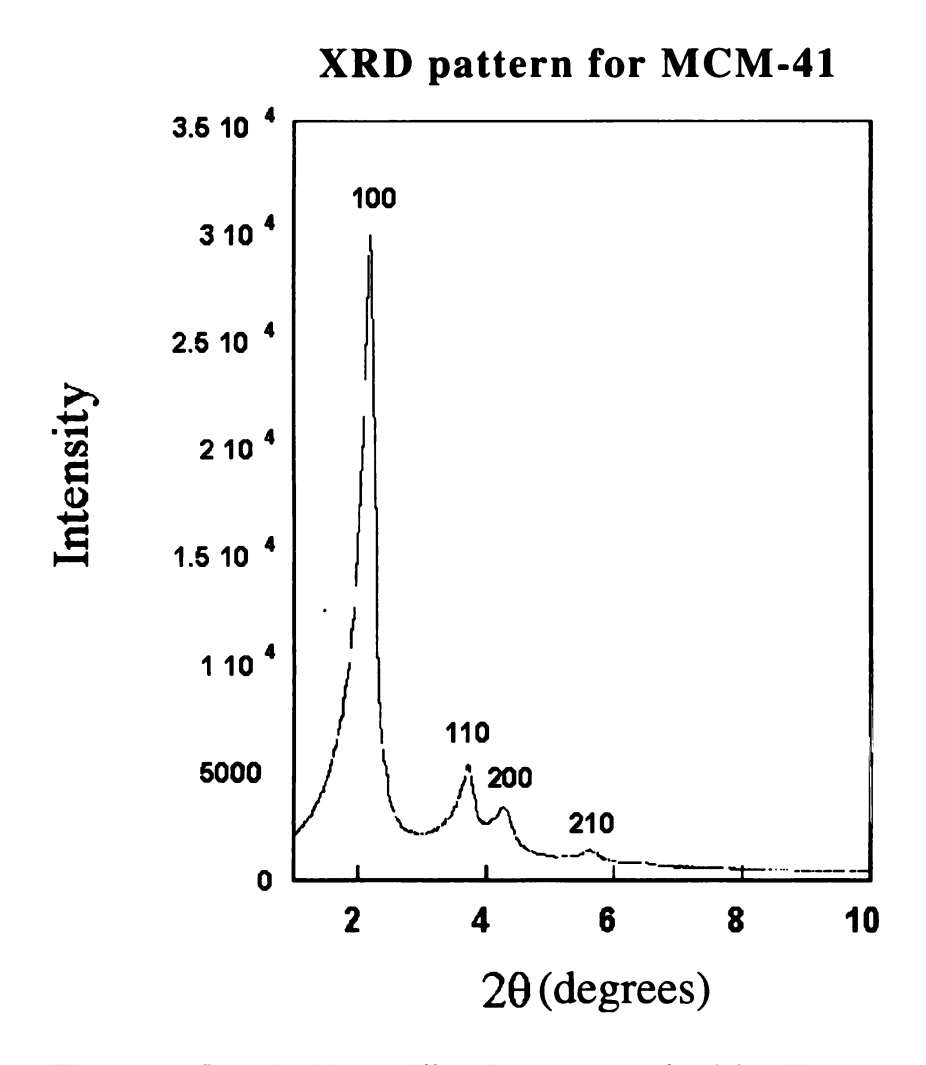


Figure 1.2 Powder X-ray diffraction pattern of calcined hexagonal MCM-41

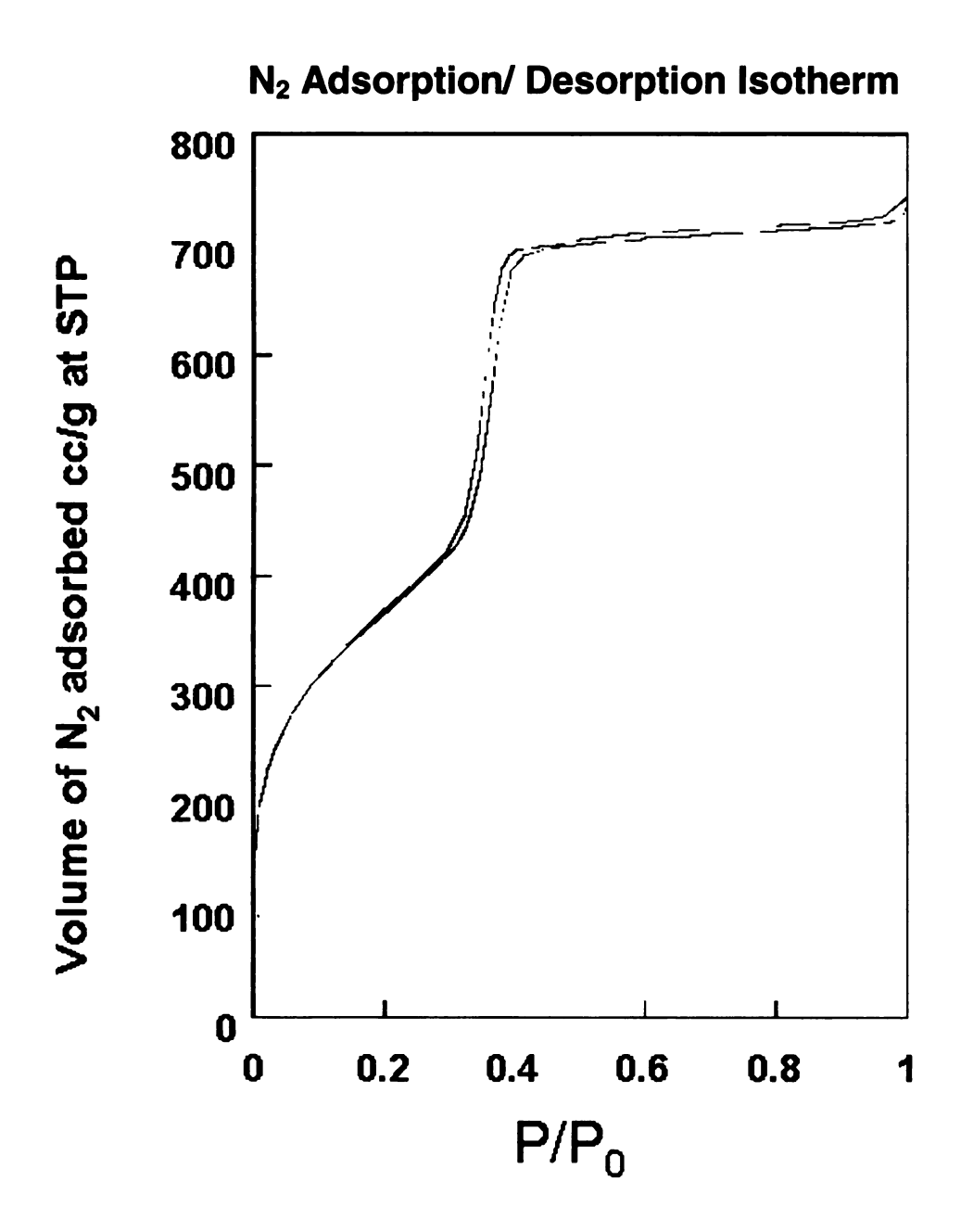


Figure 1.3 N₂ adsorption-desorption isotherm of calcined MCM-41

1.2.2 Additional Electrostatic Assembly Pathways

Stucky and co-workers¹⁴ extended the electrostatic approach to the synthesis of mesostructured materials by categorizing four specific electrostatic assembly pathways. Pathway 1 (S⁺I⁻) involves the electrostatic interaction between the cationic surfactant micelle (S⁺) and the anionic inorganic species (I⁻), proposed by Mobil¹⁰. Pathway 2 (S⁻I⁺) the charge reversal case where an anionic template (S⁻) was used to direct the assembly of cationic inorganic species (I⁺). Pathway 3 (S⁺X⁻I⁺) and Pathway 4 (S⁻X⁺I⁻) utilize a counter ion mediated route. For example Pathway 3 may use halogen ion (X⁻) to mediate interaction between the cationic silica species which occur in strongly acidic (pH < 2) solution and cationic surfactant species¹⁴. Mesoporous silica synthesized by this pathway are designated SBA materials¹⁵. Pathway 4 uses alkali metal cations as the mediating counter ions.

1.2.3 Neutral (S⁰I⁰) Assembly Pathway to Mesoporous Molecular Sieves

Tanev and Pinnavaia introduced an additional pathway into the assembly of mesoporous silicas by hydrogen bonding interactions between the surfactant micelles and silica species as the structure directing driving force (S⁰I⁰)¹⁶. In this pathway, micelles of electronically neutral long chain primary alkylamine (S⁰) are used as the structure directing species and tetraethylorthosilicate (TEOS) as inorganic precursor (I⁰) resulting in structures with thicker framework walls and improved stability. The material so formed is designated as HMS.¹⁶.

1.2.4 Non-ionic Assembly Pathway to Mesoporous Molecular Sieves

The hydrogen bonding approach was further extended by Bagshaw et al to include the bonding between non-ionic polyethylene oxide (PEO) based surfactants (N⁰) and inorganic precursors (I⁰) to form MSU-X silicas^{17,18}. Amphiphilic PEO based surfactants have hydrophilic ethylene ether - (CH₂CH₂O)- segments connected to hydrophobic R groups of varying lengths and functionality depending on the type of surfactant used. The R group could be an alkyl group as in the case of Brij and Tergitol surfactants or could be a phenyl group as in case of IGEPAL-RC and TRITON-X surfactants. The H-bonding between the surfactant and the inorganic precursor is responsible for the formation of the mesoporous molecular sieve. PXRD and N₂ adsorption-desorption isotherms give similar results to both HMS and MCM-41.

1.3 Advances in Mesoporous Molecular Sieves

1.3.1 Low pH conditions with PEO based surfactants

Recently Stucky and co-workers assembled mesoporous materials via pathway 3 i.e., (S⁺X⁻I⁺) by using PEO based surfactants and inorganic precursor like TEOS at pH conditions near the isoelectric point of silica (pH~2)^{19,20}. At these pH values the silica source hydrolyzes into silicic acid and the PEO surfactants have the hydronium ion associated with them leading to the formation of a variety of mesophases via the electrostatic pathway (N⁰H⁺)(X⁻I⁺) depending on the choice of surfactant used²⁰.

The high acid, low pH synthesis in the presence of high molecular weight tri-block co-polymer surfactants of the Pluronic series results in the formation of materials designated as SBA-15. SBA-15 mesoporous materials have hexagonal symmetry and pore diameters in the range of 25nm which are much larger then that previously attainted for other mesoporous materials ¹⁹. Also, the addition of organic swelling agents resulted in the formation of foam like materials designated as Mesostructured Cellular Foams (MCF) with pore diameter greater then 35nm. The key to this synthesis is the formation of microemulsions, which act as templates²¹.

1.3.2 Synthesis of Stable Mesostructured Silica from PEO Surfactants and Soluble Silica Sources

Guth and coworkers reported the synthesis of mesostructured silica using low cost water soluble sodium silicate as the silica source and the surfactant Triton-X 100 as the structure directing species^{22,23}. The mesostructures so formed gave X-ray diffraction patterns and pore structures similar to the MSU-X silicas. The structure was however stable only upto the calcination temperature of 480 °C, and hence removal of the surfactant at 600 °C led either to extensive restructuring of the silica or formation of an amorphous material as indicated by loss of mesoporosity.

Pinnavaia and co-workers have recently reported the assembly of mesoporous silicas with various topologies ranging from wormhole like disordered²⁴ to hexagonally ordered pore structures²⁵ synthesized using PEO

surfactants and water soluble sodium silicate. In contrast to the materials synthesized by Guth these materials are stable to the removal of surfactant by calcination leaving behind accessible pore volumes. The success of this method relies on the use of acid to neutralize the hydroxide content of the silicate in the presence of the structure directing surfactant assemblies resulting in the assembly of the mesostructures at a near neutral pH conditions. The framework pore topology can be either disordered wormhole like conventional MSU-X silicas assembled via N°1° pathway and designated MSU-X', or ordered crystalline phases similar to silicas assembled via the electrostatic pathway and designated as MSU-H silicas¹⁷. The final pore topology depends on the surfactant, auxiliary reagents and temperatures used during the synthesis.

1.4 Functionalization

Heavy metals particularly mercury and lead are important environmental pollutants, and pose a great danger to human health and natural ecosystems. Removal of these species from the environment is a major focus of waste treatment and remediation efforts. Several adsorptive compounds can capture metal ions from solutions including activated charcoal²⁶, zeolites^{27,28}, and clays^{29,30}. Inherent disadvantages of these materials are their low loading capacities and relatively low binding constants.

Chelating ligands such as thiol, amine or crown ether when coupled to support matrices consisting of inorganic oxides (silica, alumina, clay)³¹⁻⁴⁷ or organic polymers (polystyrene, cellulose or polymethylmethacralate)⁴⁸⁻⁵³ proved to be good heavy metal sorbents. These functionalized materials have high binding capacities and strong binding affinities for selected metal ions. This

exceptional performance can be attributed to the presence of the surface bound ligands, which can be specifically tuned to accommodate the selective adsorption of targeted metal ions. Although superior in performance to conventional ion exchangers, functionalized matrices remain relatively inefficient because only the fraction of the immobilized ligands are accessible for metal complexation, due to their small and irregular pore structure. Metal oxides with large uniform pore structures such as those exhibited by mesoporous molecular sieves, are expected to improve access to the ligand sites.

The internal surfaces of the mesoporous materials are reactive due to the presence of surface hydroxyl groups. These hydroxyl groups can be used to attach a number of functional groups. Surface modification of mesoporous materials can be achieved by various techniques like grafting, co-condensation of framework precursors, intra channel reaction etc⁵⁴.

Functional group can be classified into three categories

- (1) Transition metal or p-block metals which can act as Lewis acids e.g. Al, Ti, V, Cr, Mn⁵⁵⁻⁵⁹
- (2) Transition metal complexes mostly used as homogeneous catalyst such as Mn (Salen)⁶⁰, Pd (C₂H₅)⁶¹, Mn (bipy)⁶²
- (3) Organic ligands like mercaptopropyl, aminopropyl. 63

Functionalization of mesoporous materials can be achieved using two general strategies

- (1) Post synthesis grafting
- (2) Direct or co-assembly

Post synthesis grafting consists of reacting an organosilane with the silica surface using an appropriate solvent under reflux conditions. The grafting reaction uses the free silanol groups (Si-OH) present on the silica surface figure 1.4 are the schematic representation of the grafting approach.

A drawback of the grafting approach is the inability to adequately control the loading of the anchored guest species. Moreover, the steps required to obtain the functionalized product are somewhat extensive. For instance, the complete drying of both the mesostructure and the reaction solvent prior to the grafting reaction in order to avoid the formation of unwanted poly-condensation byproducts. Hexagonal MCM-41 and wormhole like HMS silicas were the first to be thiol functionalized by the grafting of 3-mercaptopropyltrimethoxysilane (3-MPTMS) a potent ligand for heavy metal ion binding⁶⁴⁻⁶⁸. These materials labeled FMMS⁶⁵ and MP-HMS⁶⁴ exhibited unprecedented high loading capacities for mercury (Hg²⁺) (2.5mmol/g and 1.5mmol/g respectively).

Unlike most other chelating adsorbents both these materials were able to bind Hg²⁺ ions to every thiol group in their structure, which is attributed to the open framework mesoporosity in the hybrid materials that allowed unhindered access of the metal ions to the binding sites.⁶⁴

12

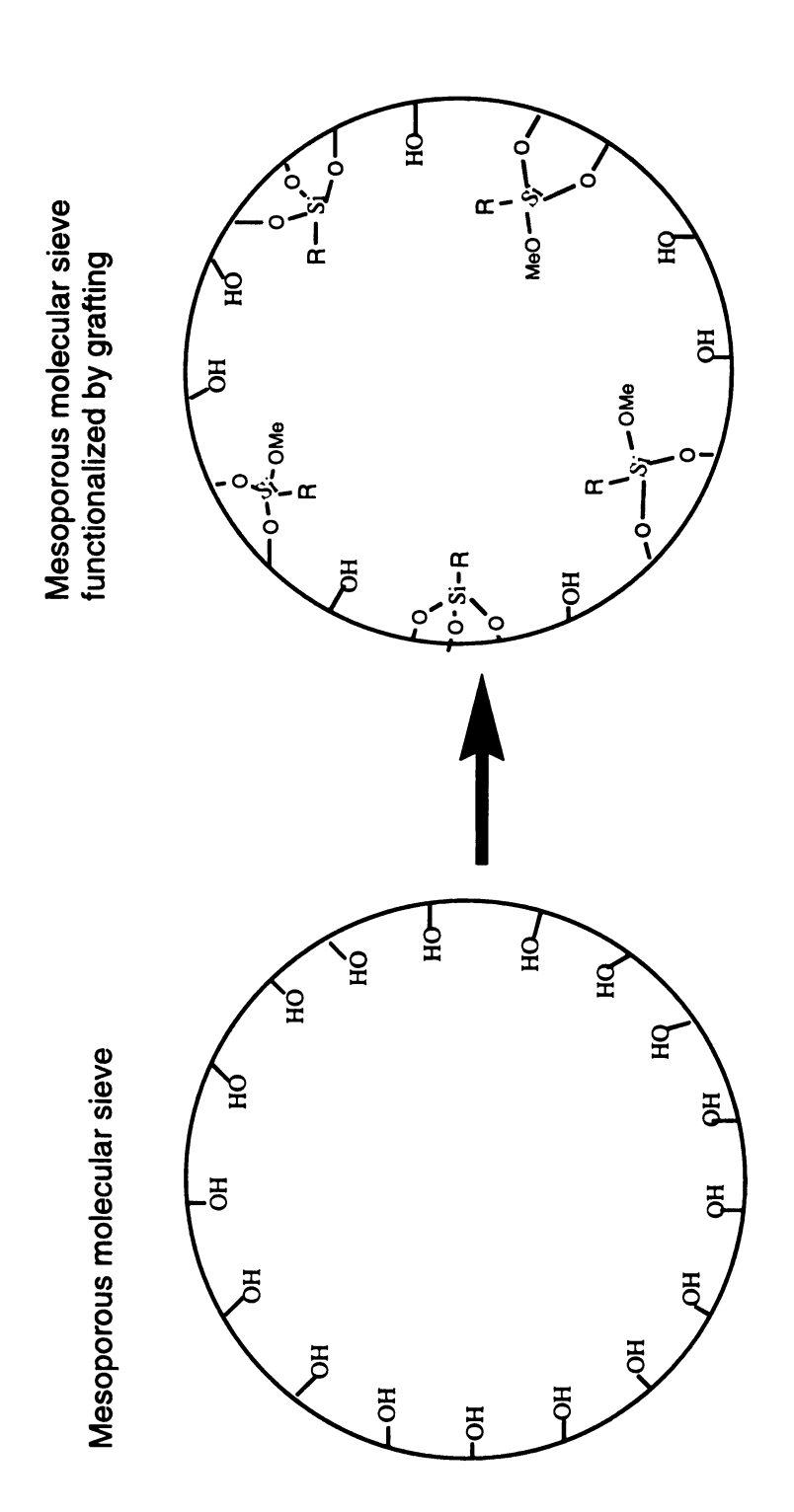


Figure 1.4 Schematic representation for the grafting of Organosilane on mesoporous molecular sieve

Direct or co-assembly method is a one step process involving the co-condensation of the siloxane and the organosilane precursors during the synthesis of mesoporous materials, figure 1.5 is the schematic representation of the direct assembly method. Direct assembly results in the uniform distribution of the organosilane groups leading to a more stable linking to the framework. To ensure the incorporation of the organosilane into the framework of the mesopores material it is important that there is no phase separation of the reagents. One of the drawbacks of the direct assembly is that, alkoxysilanes need to be used as organosilane reagents, which are expensive.

Burkett et al were the first to report the one step synthesis of hybrid organic-inorganic during the synthesis of MCM-41.⁶⁹ Although the authors demonstrated the incorporation of organic groups into MCM-41 framework, in some instances the functionalized mesostructure decomposed upon removal of the templating surfactant from the pores through acid leaching. This was explained to be the difficulty associated with the removal of the charged surfactant from the framework by extraction techniques.

Macquarrie⁷⁰ and Corriu et al⁷¹ and Bossaert et al⁷² utilized the S⁰l⁰ (HMS) and later on Richer and Mercier⁷³ utilized the N⁰l⁰ (MSU-X) assembly strategy to successfully synthesize hybrid materials, which are stable to the removal of the surfactant by extraction techniques. Thus the non-electrostatic templating technique is a convenient method for the direct synthesis of functionalized mesoporous molecular sieves.

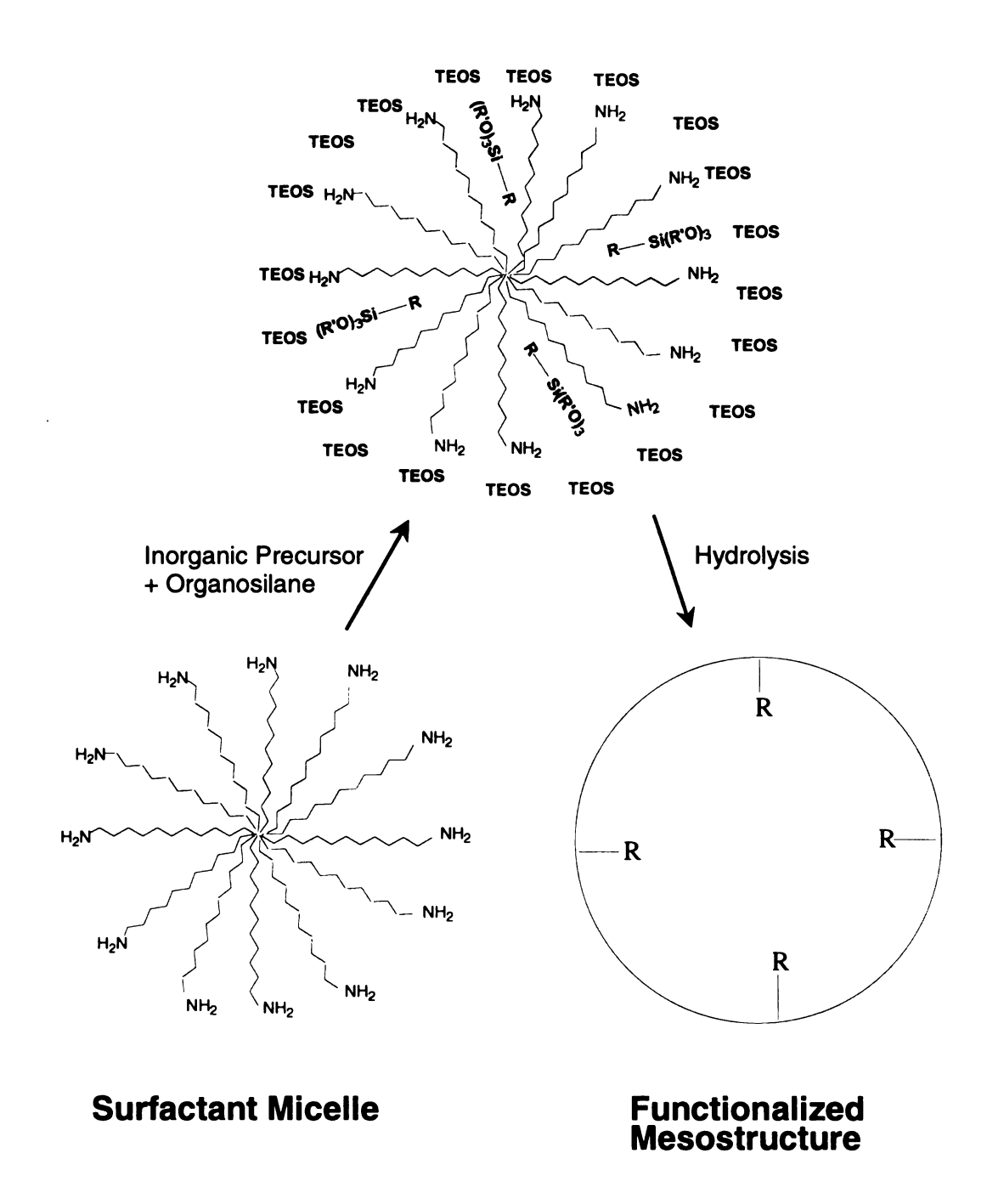


Figure 1.5 Schematic representation of mesoporous molecular sieve functionalized by direct synthesis

1.5 Research Objectives:

The synthesis of current hybrid organic-inorganic mesoporous molecular sieves is by direct assembly using tetraethylorthosilicate (TEOS) as the inorganic precursor, which is expensive. To allow for the widespread application of these materials alternative cost effective means need to be found. Also with modern environmental restrictions, in consonance with green chemistry use of biodegradable and non-toxic starting materials is attractive.

The objective of my research is to directly assemble functionalized mesoporous molecular sieves using effective water-soluble sodium silicate as the inorganic precursor and biodegradable non-toxic neutral non-ionic surfactants.

1.6 References:

- (1) Davies, M. E. Chem. Ind. 1992, 137-139.
- (2) Coma, A. Proc. VIIIth. Zeolite Conf., Eds. P. A. Jacobs and R.A. van Santen, Elsevier, Amsterdam 1989, 49.
- (3) Satterfield, C. N. Heterogeneous Catalysis in Practice, McGraw-Hill, New York 1980.
- (4) Bergna, H. E. The Colloid Chemistry of Silica, Adv. Chem. Ser., ACS, Washington, D.C. 1994, 234.
- (5) Sing, K. S. W.; Everett, D. H.; Haul, R. A. W.; Moscou, L.; Pierotti, R. A.; Rouquerol, J.; Siemieniewska, T. *Pure Appl. Chem.* **1985**, *57*, 603-619.
 - (6) Milton, R. M. 1959.
 - (7) Ching, C. B., Ruthven, D.M. Ind. Eng. Chem. Res 1987, 26, 1047.
 - (8) Roland, E. Stud. Surf. Sci and Catal 1989, 46, 645.
 - (9) Corma, A., Martinez, A. Adv. Mater. 1995, 7, 137.
- (10) Beck, J. S., Vartuli, J.C., Roth, W.J., Leonowicz, M.E., Kresge, C.T., Schmitt, K.D., Chu, C.T-W., Olson, D.H., Sheppard, E.W., McCullen, B., Higgins, J.B., Schlenker, J.L. *J. Am. Chem. Soc.*, **1992**, *114*, 10834.
- (11) C.T.Kresge, M. E. L., W.J.Roth, J.C.Vartuli, J.C.Beck *Nature* **1992**, *359*, 710.
- (12) V.Luzzati D. Chapman, Ed (Academic, New York, 1968) 1968, 71-123.
 - (13) Horvath, G.; Kawazoe, K. J. Chem. Eng. Jpn. 1983, 16, 470-475.

- (14) Q.Huo, D. I. M., U.Ciesla, P. Feng, T.E. Gier, P.Sieger, R.Leon, P.M.Petroff, F. Schuth, G.D.Stucky *Nature* **1994**, *368*, 317.
 - (15) Q.Huo, R. L., P.M.Petroff, G.D.Stucky *Science* **1995**, *268*, 1324.
 - (16) Tanev, P. T.; Pinnavaia, T. J. Science 1995, 267, 865-867.
- (17) Bagshaw, S. A.; Prouzet, E.; Pinnavaia, T. J. *Science* **1995**, *269*, 1242-1244.
- (18) Bagshaw, S. A.; Pinnavaia, T. J. *Angew. Chem.-Int. Edit. Engl.* **1996**, *35*, 1102-1105.
- (19) D.Zhao, J. F., Q. Hou, N.Melosh, G.H.Fredrickson, B.F.Chmelka, G.D.Stucky *Science* **1998**, *279*, 548.
- (20) D.Zhao, J. F., Q. Hou, B.F.Chmelka, G.D.Stucky *J. Am. Chem. Soc.*, **1998**, *120*, 6024.
- (21) Schmidt-Winkel, P.; Lukens, W. W.; Yang, P. D.; Margolese, D. I.; Lettow, J. S.; Ying, J. Y.; Stucky, G. D. *Chem. Mat.* **2000**, *12*, 686-696.
 - (22) L.Sierra, a. J.-L. G. *Microporous Mesoporous Mat.* **1999**, *27*, 243.
 - (23) L.Sierra, B. L., J.Gil and J-L Guth *Adv. Mater.* **1999**, *11*, 307.
 - (24) S-S. Kim, T. R. P., T.J.Pinnavaia *Chem. Commun.* **2000**, *835*.
 - (25) S-S. Kim, T. R. P., T.J.Pinnavaia Chem. Commun. 2000, 1661.
- (26) Faust, S. D., Ali,O.M. Chemistry of Water Treatment, Butterworth, Boston. 1983.
- (27) Huang, C. P.; Hao, O. J. Environmental Technology Letters 1989, 10, 863-874.

- (28) Zamzow, M. J., Eichbaum, B.R., Sandgren, K.R., Shanks, D.E. Separation Science Technology 1990, 25, 1555-1569.
- (29) Sikalidis, C. A.; Alexiades, C.; Misaelides, P. *Toxicological and Environmental Chemistry* **1989**, *20-1*, 175-180.
- (30) Keizer, P., Bruggenwert, M. G. M. *NATO ASI Ser. E* **1991**, *190*, 177-203.
 - (31) Layden, D. E., Luttrell, G.H. Anal. Chem. 1975, 47, 1612-1617.
- (32) Kudryavtsev, G. V.; Miltchenko, D. V.; Yagov, V. V.; Lopatkin, A. A. J. Colloid Interface Sci. 1990, 140, 114-122.
- (33) Kubota, L. T.; Moreira, J. C.; Gushikem, Y. *Analyst* **1989**, *114*, 1385-1388.
- (34) Skopenko, V. V.; Samoilenko, V. M.; Movchan, O. G. *Zhurnal Neorg. Khimii* **1982**, *27*, 1463-1465.
 - (35) Moreira, J. C.; Gushikem, Y. Anal. Chim. Acta 1985, 176, 263-267.
- (36) Moreira, W. C.; Gushikem, Y.; Nascimento, O. R. *J. Colloid Interface Sci.* **1992**, *150*, 115-120.
- (37) Gushikem, Y.; Moreira, J. C. *J. Colloid Interface Sci.* **1985**, *107*, 70-74.
- (38) Howard, A. G.; Volkan, M.; Ataman, D. Y. *Analyst* **1987**, *112*, 159-162.
- (39) Volkan, M.; Ataman, O. Y.; Howard, A. G. *Analyst* **1987**, *112*, 1409-1412.
 - (40) Iamamoto, M. S.; Gushikem, Y. Analyst 1989, 114, 983-985.

- (41) Iamamoto, M. S.; Gushikem, Y. *J. Colloid Interface Sci.* **1989**, *129*, 162-165.
- (42) Izatt, R. M.; Bradshaw, J. S.; Bruening, R. L. *Pure Appl. Chem.* **1996**, *68*, 1237-1241.
- (43) Tikhomirova, T. I.; Fadeeva, V. I.; Kudryavtsev, G. V.; Nesterenko, P. N.; Ivanov, V. M.; Savitchev, A. T.; Smirnova, N. S. *Talanta* **1991**, *38*, 267-274.
- (44) Andreotti, E. I. S.; Gushikem, Y. *J. Colloid Interface Sci.* **1991**, *142*, 97-102.
- (45) Dias, N. L.; Gushikem, Y.; Polito, W. L. *Anal. Chim. Acta* **1995**, *306*, 167-172.
- (46) Dias, N. L.; Gushikem, Y.; Rodrigues, E.; Moreira, J. C.; Polito, W.L. J. Chem. Soc.-Dalton Trans. 1994, 1493-1497.
 - (47) Mercier, L. Can. Min. J. 1999, 120, 6-7.
 - (48) Phillips, R. J.; Fritz, J. S. Anal. Chem. 1978, 50, 1504-1508.
 - (49) Sugii, A.; Ogawa, N.; Hashizume, H. *Talanta* **1980**, *27*, 627-631.
 - (50) Deratani, A.; Sebille, B. *Anal. Chem.* **1981**, *53*, 1742-1746.
- (51) Alexandratos, S. D.; Wilson, D. L. *Macromolecules* **1986**, *19*, 280-287.
 - (52) Tzeng, D. L.; Shih, J. S.; Yeh, Y. C. *Analyst* **1987**, *112*, 1413-1416.
- (53) Kantipuly, C.; Katragadda, S.; Chow, A.; Gesser, H. D. *Talanta* **1990**, *37*, 491-517.
 - (54) Moller, K.; Bein, T. Chem. Mat. 1998, 10, 2950-2963.

- (55) Tanev, P. T.; Chibwe, M.; Pinnavaia, T. J. *Nature* **1994**, *368*, 321-323.
- (56) Hamdan, H.; Bailey, A.; Martinez, J. J.; Fenwick, R.; Leon, J. A. Clin. Chem. 1996, 42, 7-7.
- (57) Reddy, K. M.; Moudrakovski, I.; Sayari, A. *J. Chem. Soc.-Chem. Commun.* **1994**, 1059-1060.
 - (58) Ulagappan, N.; Rao, C. N. R. *Chem. Commun.* **1996**, 1047-1048.
- (59) Zhao, D. Y.; Goldfarb, D. *J. Chem. Soc.-Chem. Commun.* **1995**, 875-876.
 - (60) Kim, G. J.; Kim, S. H. Catal. Lett. 1999, 57, 139-143.
 - (61) Mehnert, C. P.; Ying, J. Y. Chem. Commun. 1997, 2215-2216.
- (62) Kim, S. S.; Zhang, W. Z.; Pinnavaia, T. J. Catal. Lett. 1997, 43, 149-154.
- (63) Fowler, C. E.; Burkett, S. L.; Mann, S. *Chem. Commun.* **1997**, 1769-1770.
 - (64) Mercier, L.; Pinnavaia, T. J. Adv. Mater. 1997, 9, 500-&.
- (65) Feng, X.; Fryxell, G. E.; Wang, L. Q.; Kim, A. Y.; Liu, J.; Kemner, K.M. Science 1997, 276, 923-926.
 - (66) Lim, M. H.; Blanford, C. F.; Stein, A. Chem. Mat. 1998, 10, 467-+.
- (67) Mercier, L.; Pinnavaia, T. J. *Environ. Sci. Technol.* **1998**, *32*, 2749-2754.
- (68) Brown, J.; Mercier, L.; Pinnavaia, T. J. *Chem. Commun.* **1999**, 69-70.

- (69) Burkett, S. L.; Sims, S. D.; Mann, S. *Chem. Commun.* **1996**, 1367-1368.
 - (70) Macquarrie, D. J. Chem. Commun. 1996, 1961-1962.
- (71) Corriu, R. J. P.; Mehdi, A.; Reye, C. *Comptes Rendus Acad. Sci. Ser. II C* 1999, *2*, 35-39.
- (72) Bossaert, W. D.; De Vos, D. E.; Van Rhijn, W. M.; Bullen, J.; Grobet, P. J.; Jacobs, P. A. *J. Catal.* **1999**, *182*, 156-164.
 - (73) Richer, R.; Mercier, L. Chem. Commun. 1998, 1775-1776.

Chapter 2

Synthesis of functionalized mesoporous silicas from nonionic surfactants and water-soluble silicas

2.1 Introduction:

Since the discovery of M41S materials in 1992 by Mobil researchers a great deal of attention has been given to supramolecular assembly of mesoporous materials. To date, the synthesis of mesoporous materials can be classified into several general pathways according to their organic-inorganic interfacial interactions. Electrostatic charge matching 1-3, H-bonding 4-7, and dative bonding interactions^{8,9} between the organic micelle inorganic interface have been utilized in the formation of mesostructured inorganic oxides. Until recently, the synthesis of mesostructured materials relied on the use of either a costly organic reagent, such as the quaternary ammonium salts used in electrostatic pathways, expensive molecular inorganic or an precursors, such as the tetraethylorthosilicate (TEOS) used in H-bonding and dative bonding pathways.

Guth and co-workers^{10,11} were the first to report the synthesis of mesostructured silica from the combination of inexpensive polyethylene oxide (PEO) based non-ionic surfactants and low cost sodium silicate as the inorganic precursor. The mesostructure so obtained was not stable to complete removal of the surfactants at calcination temperatures of 600 °C.

Pinnavaia and co-workers¹² recently reported synthesis of stable mesostructured silicas using non-ionic polyethylene based surfactants and sodium silicate as the inorganic precursor. This methodology requires the

neutralization of the hydroxide content of the silicate with an organic acid in the presence of the structure directing surfactant assemblies. Thus, the assembly of the mesostructure takes places at a near neutral pH conditions. The framework topology of the formed mesostructured material can be either a disordered wormhole analogous to conventional Nolo assembled MSU-X5 (denoted as MSU-X'), ordered hexagonal similar to materials assembled by the electrostatic pathway like SBA-15 (designated MSU-H13), or large pore foam-like materials (denoted as MSU-F13). The pore topology is dependent on the surfactant, auxiliary reagents and temperatures used in the synthesis.

The functionalization of the materials synthesized using cost effective reagents is desirable for the large-scale applications of these materials. Functionalized materials find use as catalysts, heavy metal ion traps, ion-exchangers, adsorbents, and sensory materials. Present work is an effort to achieve the above objective.

The synthesis of functionalized mesostructure by a one step direct assembly methodology requires that there is no phase separation of the reagents. This presents a challenge for the direct synthesis of functionalized materials using water- soluble sodium silicate, because the organosilane reagent and the inorganic precursor are immiscible. Hence, the synthesis process needs to be modified from the conventional MSU-X' synthesis procedure. In order to avoid phase separation of the oraganosilane reagent a concentrated acid is used to acidify the ethanol surfactant solution instead of dilute acids. Since water-soluble silica sources are used in the synthesis the sequence of addition of the

oraganosilane reagent and the silica source is also changed from the previously used procedures of direct synthesis. The organosilane reagent is added immediately to the acidified solution of the surfactant and allowed to partially hydrolyze the organosilane reagent for an hour before the addition of the silica source as opposed to the simultaneous addition of organosilane to the silica source when TEOS is used as the silica source.

In the present work alkylpoly(ethylene oxide) diblock copolymer surfactant like Brij 56 and alkyl-EO/furan surfactant like Tween 80 were used as the structure directing surfactants. 3-Mercaptopropyltrimethoxysilane was used as the organosilane reagent and sodium silicate was used as the water-soluble silica source.

Brij 56 [C₁₆H₃₃ (OCH₂CH₂)₁₀ OH]

 $R = (CH_2)_7 CH = CH(CH_2)_7 CH_3$

x+y+z+w = 20

2.2 Experimental:

The non-ionic surfactants used were Tween 80 and Brij 56, which were obtained from Aldrich. The sodium silicate and the organosilane reagent

3-mercaptopropyltrimethoxysilane (3-MPTMS) were also obtained from Aldrich.

All of the reagents were used as obtained without further purification.

2.2.1 Synthesis of MP-MSU-X' from Tween 80 and Brij 56 surfactants

and sodium silicate:

1.2 g of the surfactant was dissolved in 2.5 ml of ethanol and 0.6 g of

glacial acetic acid. The acid added was equivalent to the amount needed to

neutralize the hydroxide content of sodium silicate. Following the dissolution of

the surfactant x moles of 3-MPTMS were added and the reaction mixture stirred at

room temperature for 1hr. After 1hr (1-x) moles of sodium silicate dissolved in 35

ml deionized water was added to the reaction mixture. This mixture was shaken

for 20 hrs at 60°C in a controlled temperature water bath. The product was then

filtered and dried to room temperature and then subjected to solvent extraction

with ethanol to remove the surfactant and unreacted organosilane reagent. The

reaction stoichiometry was as follows:

Tween 80 (T80)

1-x SiO₂: (0.40-x) Na₂O: 0.073 T80: x 3-MPTMS: 0.8 Acetic acid: 3.4 Ethanol:134

Water

Brij 56 (B56)

1-x SiO₂: (0.40-x) Na₂O: 0.140 B56: x 3-MPTMS: 0.8 Acetic acid: 3.4 Ethanol:134

Water

26

2.2.2 Physical Measurements:

Wide angle powder X-ray diffraction (XRD) patterns were obtained using a Rigaku Rotaflex Diffractometer with CuK_{α} radiation ($\lambda = 0.154$ nm). Counts were accumulated every 0.02 degrees (20) at a scan speed 0.5 degrees per minute.

N₂ adsorption-desorption isotherms were obtained at -196 °C on a Micromeritics ASAP 2010 Sorptometer using standard procedures. Samples were outgassed at 100 °C and 10⁻⁶ Torr for a minimum of 12hrs prior to analysis. BET surface areas were calculated from the linear part of the BET plot according to IUPAC recommendations.¹⁴ The Horvath Kawazoe model was used to estimate pore size distributions from the adsorption branch of the isotherms.¹⁵

TEM images were obtained on a JOEL 100CX microscope with a CeB₆ filament and an accelerating voltage of 120 KV. Sample grids were prepared by sonicating samples in a ethanol for 20 min and evaporating 1 drop of the suspension onto a carbon coated, holey film supported on a 3 mm, 300 mesh copper grid.

²⁹Si MAS NMR spectra were recorded on a Varian 400 solid state NMR spectrometer at 79.5 MHz under single-pulse mode with a Zirconia rotor at a spinning frequency of 4 kHz and a pulse delay of 400 seconds.

2.3 Results and Discussion

2.3.1. Mesostructures assembled using Tween 80 surfactant:

The assembly of the mesostructured MP-MSU-X' silicas is assumed to take place by the N^0l^0 assembly mechanism.¹² In this mechanism the non-ionic surfactant (N^0) is electrically neutral and the acidified silicate is assumed to be

electrically neutral silicic acid. The synthesis is carried out at near neutral pH conditions to facilitate H-bonding interaction between the water-soluble silica species and the neutral surfactant.

Figure 2.1 shows the powder X-ray diffraction pattern for the non-functionalized and organo- functionalized MSU-X' silicas. The molar composition of the organosilica was varied from 0.05-2.5 moles, which corresponds to x values between 5 mole% and 25 mole%. All of the samples show XRD patterns typical of an MSU-X' wormhole motif mesostructures featuring a single pore-pore correlation reflection at 20 angle usually between 1° and 3°. The reduction of XRD signal intensity in these 3-MPTMS loaded mesostructures could be attributed to contrast matching between the silica framework and the incorporated 3-MPTMS groups in the samples.

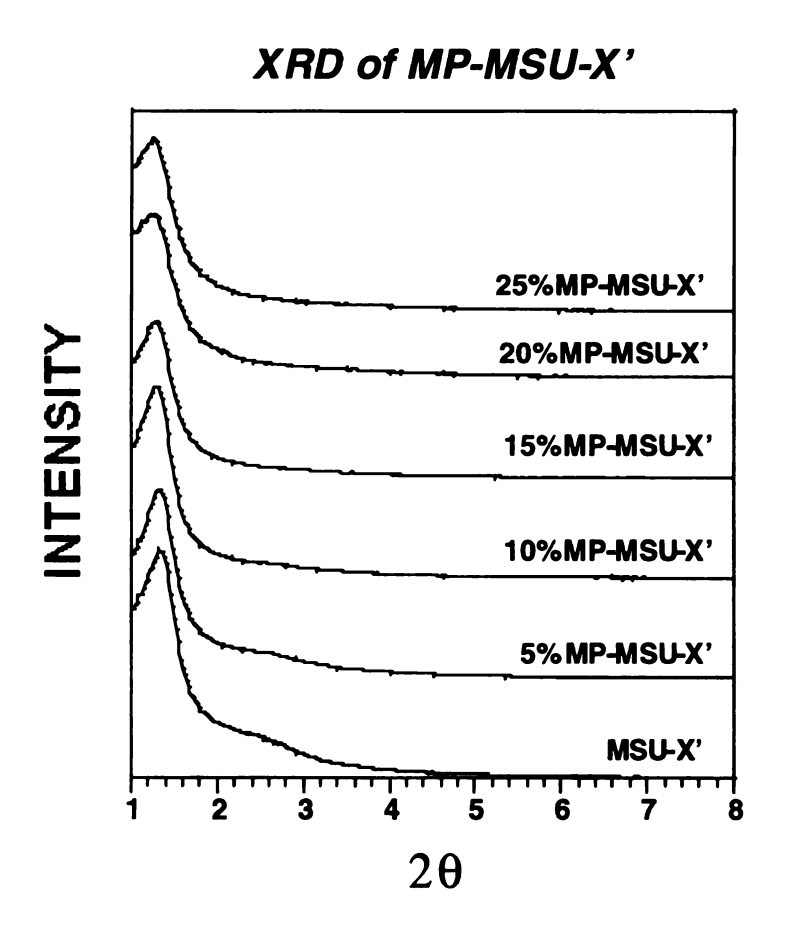


Figure 2.1 Powder X-ray diffraction pattern for 3-MPTMS functionalized MP-MSU-X' silicas synthesized using Tween 80 surfactant.

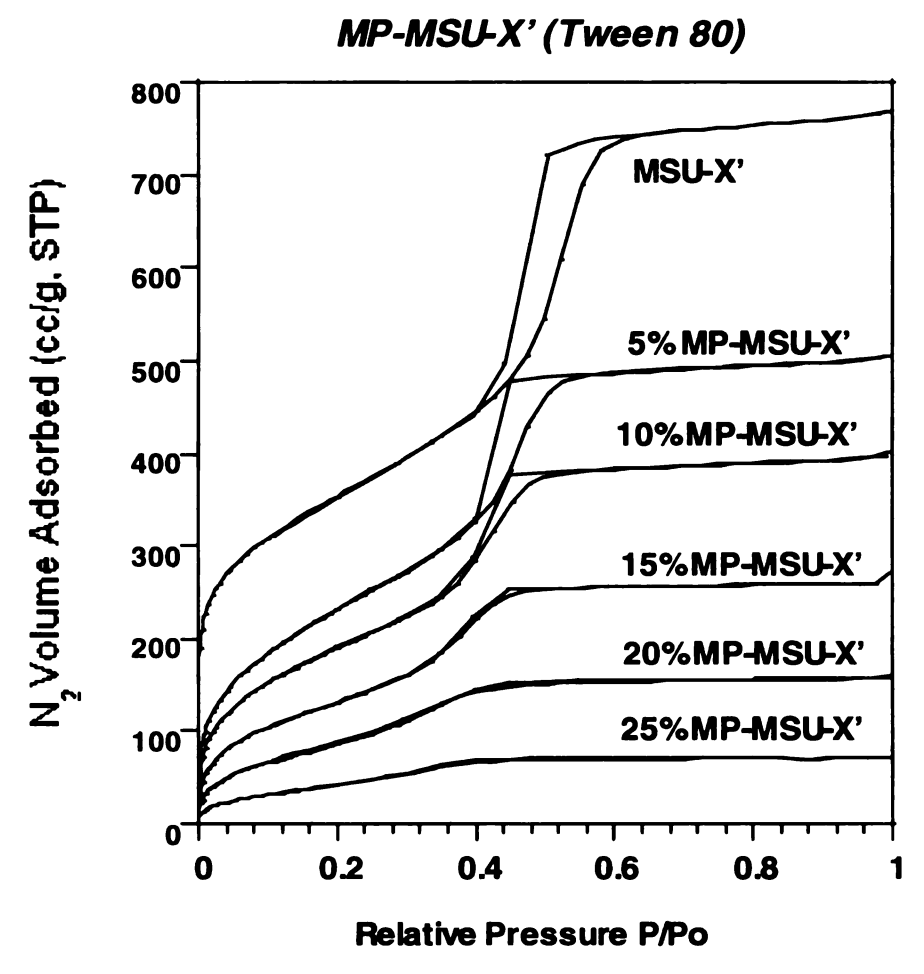


Figure 2.2 Nitrogen adsorption-desorption isotherms for mercaptopropyl functionalized silicas from x MPTMS and (1-x) sodium silicate mixtures in the presence of Tween 80 as the surfactant

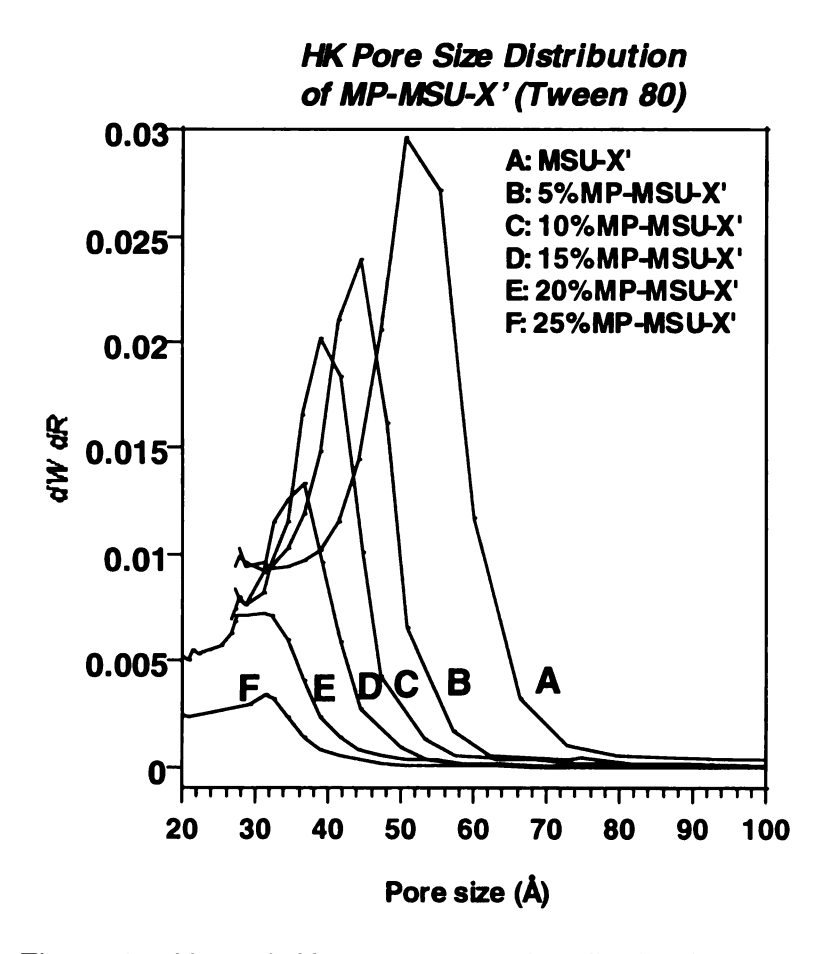


Figure 2.3 Horvath-Kawazoe pore size distributions obtained from the nitrogen adsorption isotherms of the MP-MSU-X' mesostructures described in Figure 2.2

Figures 2.2 and 2.3 illustrate the effect of increasing the functional group loading on the nitrogen isotherms of the mesostructures and the corresponding change in the pore sizes. The shift in the position of the isotherm inflections to lower partial pressures (P/Po) values denotes a systematic decrease in the pore diameters as a function of 3-MPTMS incorporation. Moreover, the pore volumes of the mesostructures also decrease concurrently with the pore diameters. This decrease in the pore diameter and the pore volume is attributed to the occupancy of the pore channels by the incorporated 3-MPTMS. An increase in the wall thickness with the increasing incorporation of 3-MPTMS also proves that the pore channels are occupied by the 3-MPTMS groups. The physical properties of the MP-MSU-X' are listed in Table 2.1

Table 2.1 Physical Properties of MP-MSU-X' (Tween 80)

Sample	d ₁₀₀	Surface area (m²/g)ª	Pore Diameter (nm) ^b	Wall Thickness (nm) ^c	Pore Volume (cm ³ /g) ^d
MSU-X′	6.7	006	5.0	1.7	1.04
5% MP-MSU-X'	6.7	829	4.4	2.3	0.80
10% MP-MSU-X	6.9	089	3.8	3.1	0.62
15% MP-MSU-X	6.9	490	3.6	3.3	0.42
20% MP-MSU-X	7.1	339	3.0	4.1	0.25
25% MP-MSU-X	7.1	163	2.5	4.6	0.11

^a Calculated by the Brunaeur-Emmett-Teller (BET) method. ^b Determined by the Horvath-Kawazoe model. ^c Wall thickness determined from the difference between d_{100} and pore diameter. ^d Pore volume determined at P/Po = 0.98

Figure 2.4 shows the ²⁹Si MAS NMR spectra for MSU-X' and MP-MSU-X'. The resonance near –95, –100 and –112 ppm represent the Q² Si(OSi)₂ (OH)₂, Q³ Si(OSi)₃OH and Q⁴ Si(OSi)₄ environments of the SiO₄ tetrahedra, whereas the –59 and –68 ppm signals arise from the T² SHCH₂CH₂CH₂-Si(OSi)₃OH and T³ SHCH₂CH₂-Si(OSi)₃ connectivity's of the 3-MPTMS functionalized silicon centers.

Table 2.2 reports the framework cross-linking parameters Q^4/Q^3 and $(Q^4 + T^3)/(Q^3 + T^2)$ for representative mesopores structures. The framework cross-linking increases with an increase in the 3-MPTMS loading. The integral intensities of the deconvoluted peaks were used to calculate the framework cross-linking and the millimoles of sulfur incorporated into the material. The degree of cross-linking is indicative of the anticipated framework stability; the greater the cross-linking, the greater the expected stability of the framework.

Figure 2.5 shows the TEM images for the MSU-X' and 20% MP-MSU-X' mesostructures. The samples clearly depict the wormhole pore structure even at high organosilane incorporation.

Table 2.2 ²⁹Si NMR Cross linking parameters for MP-MSU-X' assembled using Tween 80 surfactant

Material	Хехр	X _{cal}	Q⁴	Q ³	Q²	Q ⁴ /Q ³ +Q ²	T ³	T²	Q^4+T^3/Q $^3+Q^2+T^2$	mmol SH/g
MSU-X'	•	-	0.6	0.35	0.05	1.5	-	•	1.5	•
MP-MSU-X'	0.10	0.06	0.6	0.35	0.04	1.53	0.05	0.006	1.64	1.2
MP-MSU-X'	0.25	0.16	0.6	0.35	0.03	1.66	0.12	0.04	1.71	1.9

²⁹Si NMR of MP-MSU-X' (Tween 80)

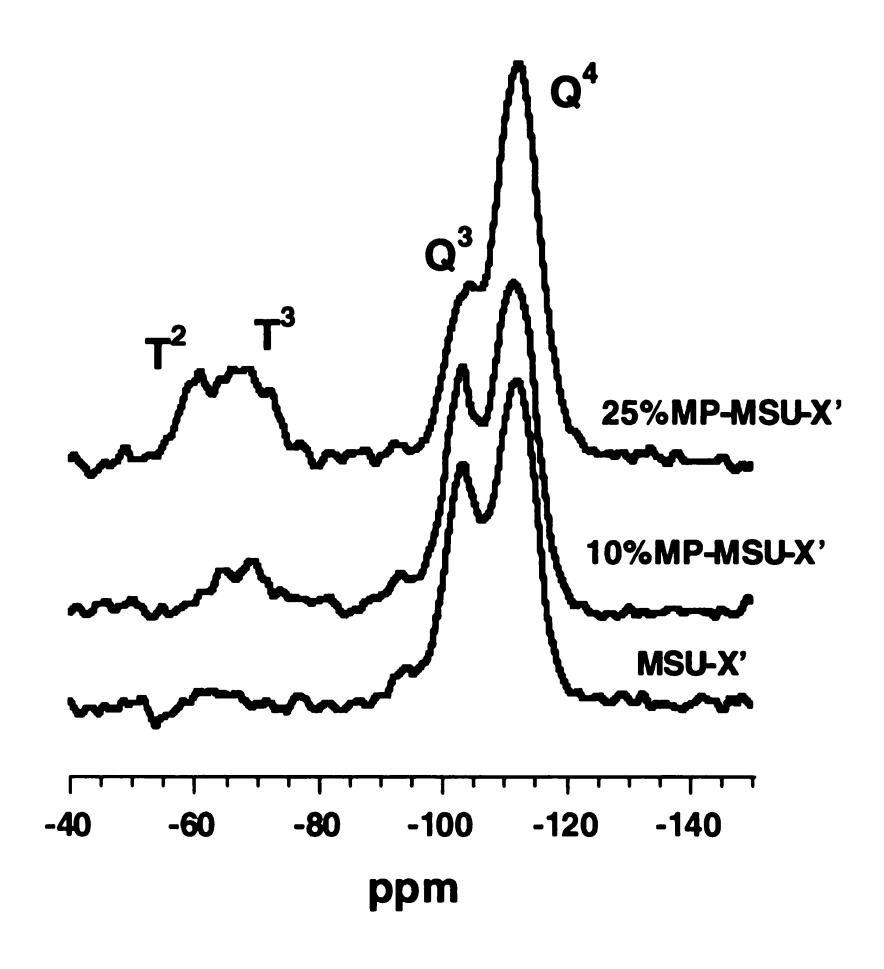


Figure 2.4 ²⁹ Si MAS NMR spectra of MP-MSU-X' assembled using Tween 80 surfactant with different moles of MP

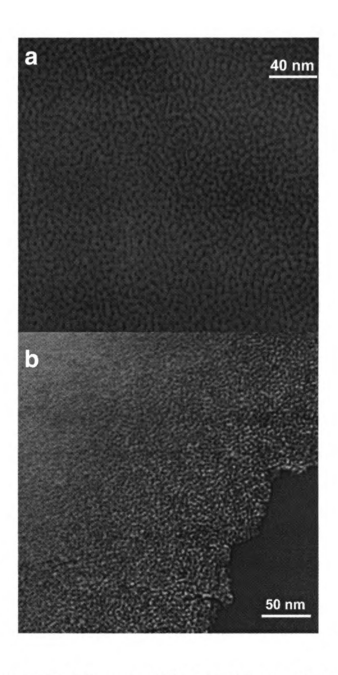


Figure 2.5 TEM images of (a) MSU-X' and (b) 20% MP-MSU-X' assembled using Tween 80 as the surfactant

2.3.2 Mesostructure assembled using Brij 56 surfactant.

Figure 2.8 is the powder X-ray diffraction pattern for the non-functionalized and organo-functionalized MSU-X' silicas assembled using Brij 56 as the surfactant. The molar composition was varied from 0.05 to 2.5 moles. Unlike mesostructures made by Tween 80 surfactant which showed only one peak, mesostructures assembled by Brij 56 depicted an X-ray pattern with at least three reflections that strongly suggested the formation of the hexagonally ordered pores. The d_{100} reflections of the various materials were significantly more narrow and intense than materials prepared under neutral non-ionic conditions. The strong intensities of the d_{100} reflections relative to the d_{110} and d_{200} peaks indicated that the samples did not contain 100% hexagonally ordered pore architectures. The hexagonal order was lost at higher 3-MPTMS loading (x = 0.20) and reverted to a single peak reminiscent of a wormhole pattern. Figure 2.9 are the TEM images showing the bimodal pore structures for the materials assembled using Brij 56 surfactant.

Electrolytes added to the surfactant emulsions can affect the aggregation characteristics of both ionic and non-ionic surfactants¹⁶. Additionally, electrolytes can modify the rate and extent of silicon alkoxide hydrolysis and condensation¹⁷. These effects were recently exploited in the MSU-X system by Bagshaw¹⁸ and Pinnavaia et al.^{12,13,19} and Prouzet et al.^{7,20} who separately reported the formation of bimodal pore systems, hexagonally ordered pores and controlled particle morphologies, respectively, through the modifications of the ionic strength of the MSU-X synthesis media.

These reports, together with the present results show that highly ordered pore structures are readily formed form neutralized sodium silicate solutions. The highly symmetrical pores and hexagonal framework produced from solutions with high sodium ion concentrations strongly indicate that a cation structure directing effect is operating. Long-range electrostatic forces acting between the surfactant micelles are expected to facilitate ordering of the resulting mesostructure into a hexagonal, cubic, or lamellar framework¹⁹. However, the detailed mechanisms of this structure direction are unclear. Bagshaw recently postulated two separate or closely related possibilities²¹.

Spectroscopic investigations of the PEO-based surfactant interactions with a series of alkali and alkali-earth cations have shown that the metal cations interact with the ethylene oxide functions creating TTGTTG (T = trans, G = gauche) series of conformations. This creates helical crown ether like metal PEO complexes²². In the silicate templating environment this complexation caused the H-bonding sites to become unavailable for templating or silicate hydrolysis. Also, metal ion complexation by the PEO groups causes the H-bonding sites to be directed into the interior of the now helical PEO/M+ headgroup. Thus, the previously nucleophilic EO units are no longer available for H-bonding to silica species at the micelle-surfactant interface, but electrostatic forces are now present between micelles, which helps to induce long-range order. One of the possibilities for PEO-M+ coordination could be that one or two metal cations complex with the first two or three EO units. This leads to a gauche

Table 2.3 X-ray diffraction values for MP-MSU-X' mesostructures assembled using Brij 56 surfactant

Experi	mental		Calcula	ated	
d ₁₀₀	d ₁₁₀	d ₂₀₀	d ₁₀₀	d ₁₁₀	d_{200}
58.1	33.1	29.3	58.1	33.5	29.1
57.4	32.7	28.3	57.4	33.1	28.7
57.4	32.2	28.1	57.4	33.2	28.7
58.1	33.2	28.7	58.1	33.5	29.0
	58.1 57.4 57.4	58.1 33.1 57.4 32.7 57.4 32.2	d ₁₀₀ d ₁₁₀ d ₂₀₀ 58.1 33.1 29.3 57.4 32.7 28.3 57.4 32.2 28.1	d ₁₀₀ d ₁₁₀ d ₂₀₀ d ₁₀₀ 58.1 33.1 29.3 58.1 57.4 32.7 28.3 57.4 57.4 32.2 28.1 57.4	d ₁₀₀ d ₁₁₀ d ₂₀₀ d ₁₀₀ d ₁₁₀ 58.1 33.1 29.3 58.1 33.5 57.4 32.7 28.3 57.4 33.1 57.4 32.2 28.1 57.4 33.2

XRD of MP-MSU-X' (B56)

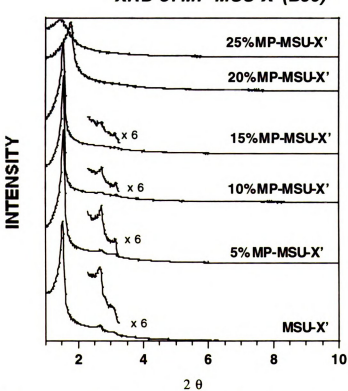


Figure 2.6 Powder X-ray diffraction patterns for MP-MSU-X' synthesized using Brij 56 surfactant

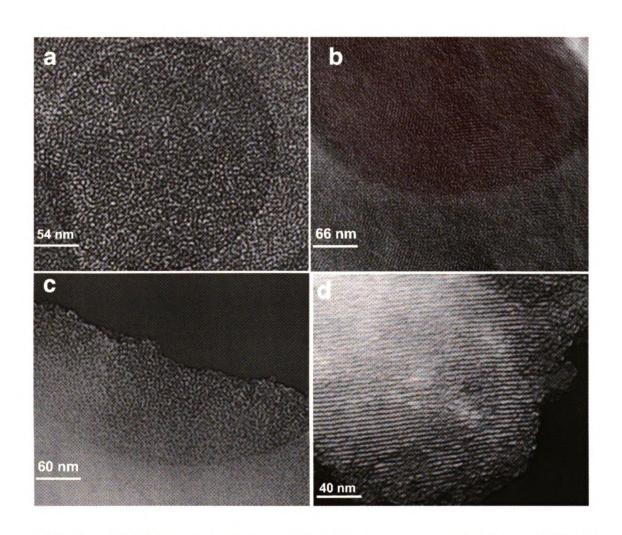
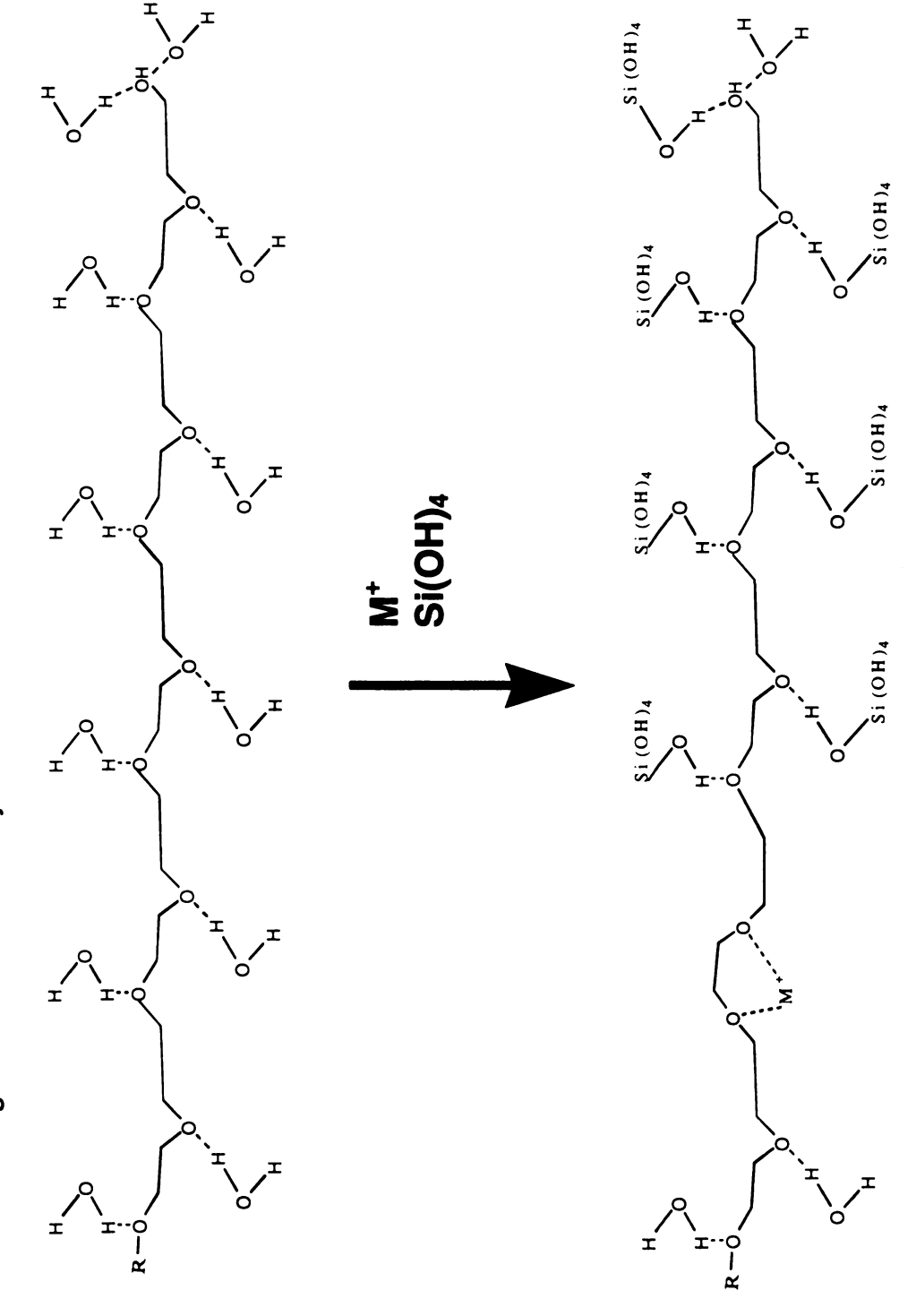


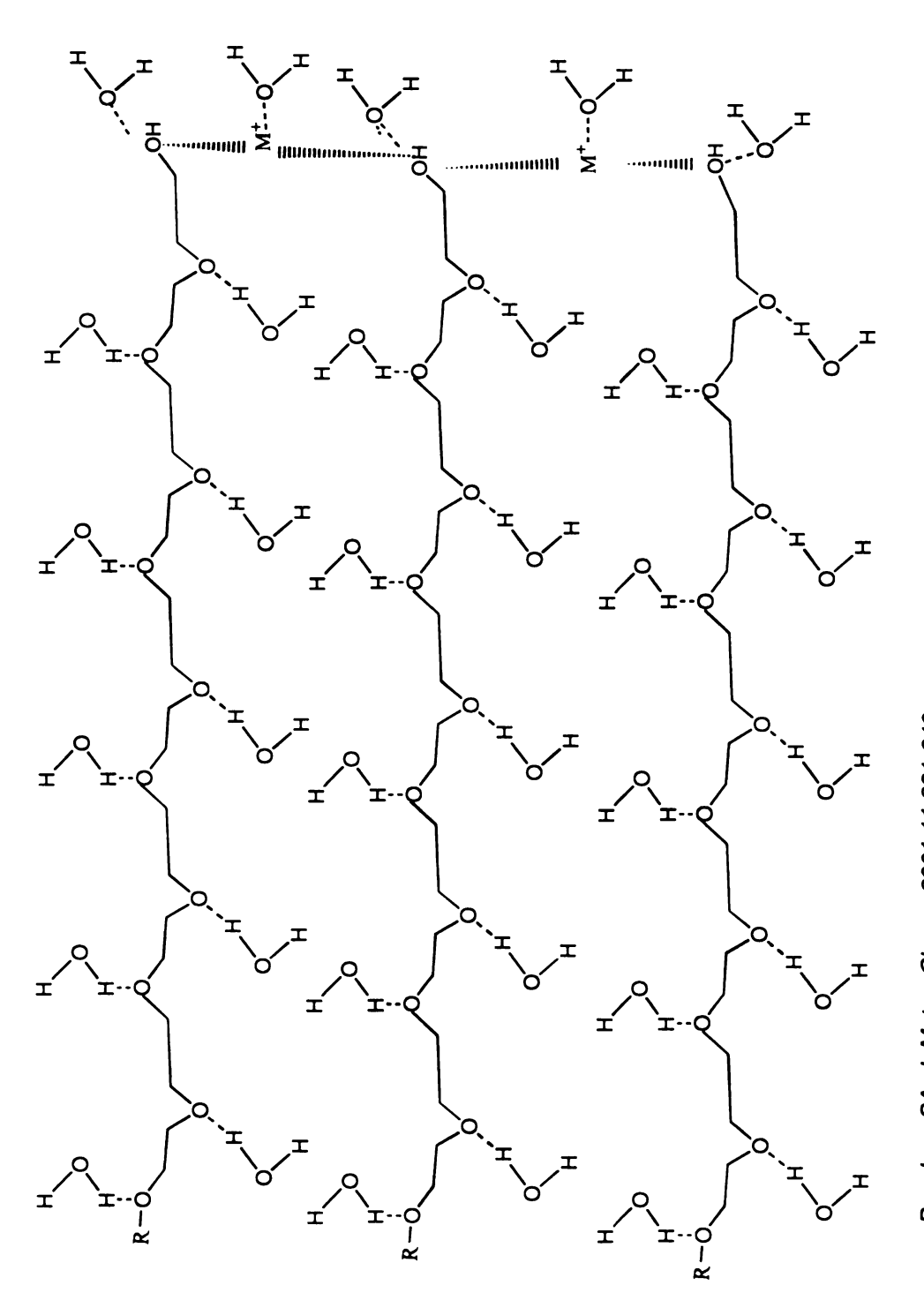
Figure 2.7 TEM images showing the bimodal pore morphology for (a, b) MSU-X' and (c, d) 15% MP-MSU-X' assembled using Brij 56 as the surfactant

Figure 2.8 Scheme1 Diagram of interaction of PEO surfactant, silica and metal cations and induction of gauche conformation by M⁺ cations



Bagshaw SA, J. Mater. Chem., 2001,11,831-840

Figure 2.9 Scheme 2 Diagram of interaction between \mathbf{M}^{\star} cations linking PEO surfactant headgroups



Bagshaw SA, J. Mater. Chem., 2001,11,831-840

conformation in the PEO chains that could cause the head group to form a "Kinked" chain and thus reducing the packing parameter g. This is depicted in Scheme 1, Figure 2.6.

Another possibility could be that the flexibility of the PEO/H⁺/silicate complex allows the headgroup packing parameter to be modified by the cation without disruption of the hydrogen bonding between the PEO headgroups and the growing silicate species. The cations will then interact with the PEO-silicate complex, which causes the surfactant head group area to decrease and the packing parameter g to increase. The result is the formation of hexagonal pore symmetry along with regions of regular wormhole like disordered pores.

A third possibility could be that the cations do not in fact modify the template microstructure, but form bridging interactions between terminal OH groups of adjacent templates leading to formation of symmetrical structures Scheme 2, Figure 2.7.

It can then be argued that the cations should homogeneously distribute throughout the templating system and give a homogeneously templated system. Siew et al state that PEO surfactants will coordinate only 3-4 alkali or alkali-earth cations for every 10 EO groups. Therefore, 5 mol % cation loading with respect to silica produces 0.4 M⁺ per R-(EO)₁₀ surfactant molecule. If all of the cations are coordinated by the surfactant as 1:4 complexes, only 10% of the surfactant molecules will interact fully with the metal cations. This explains the bimodal pore morphology.

Figure 2.10 and 2.11 show the nitrogen adsorption desorption isotherms and the Horvath Kawazoe (HK) pore size distribution for the MP-MSU-X' materials assembled using Brij 56 surfactant. Table 2.3 depicts the physical properties of the assembled materials. The data obtained showed that the hexagonally ordered pores are smaller in diameter then the wormhole pores templated under electrically neutral assembly using similar templates. This suggests that the cation interaction with the PEO headgroups also induce molecular conformation changes that reduce the effective templating length of the surfactant. As with all the organofunctionalized materials the pore diameter decreased and the wall thickness increased with higher MP functionalization.

Figure 2.12 is the ²⁹Si MAS NMR spectra for MSU-X' and MP-MSU-X'. The framework cross-linking and the mercaptan mole fractions were calculated from the deconvoluted ²⁹Si MAS NMR spectroscopic data and the results are depicted in Table 2.4. The higher the cross-linking the greater is the stability of the framework.

MP-MSU-X' (Brij 56)

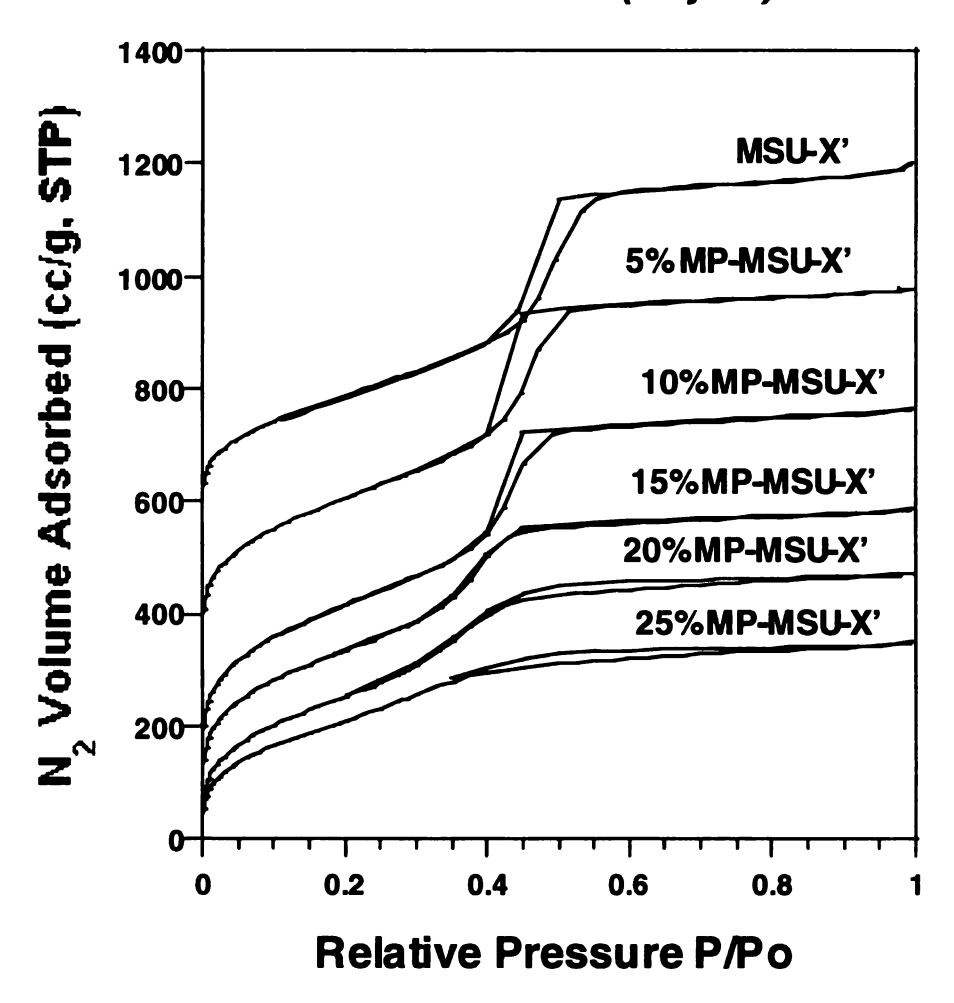


Figure 2.10 Nitrogen adsorption-desorption isotherms for mercaptopropyl functionalized silicas from xMPTMS and (1-x) sodium silicate mixtures in the presence of Brij 56 surfactant

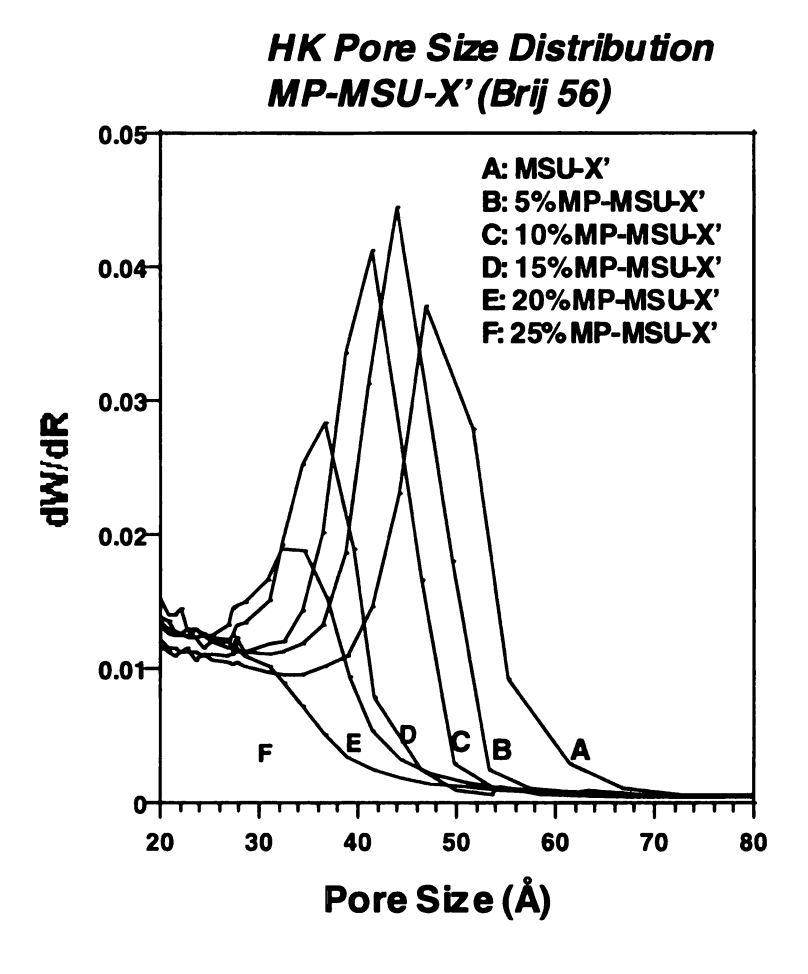


Figure 2.11 Horvath-Kawazoe pore size distributions obtained from the nitrogen isotherms of the MP-MSU-X' mesostructures described in Figure 2.8

Table 2.4 Physical properties of MP-MSU-X' assembled using Brij 56 surfactant

Sample	d ₁₀₀ (nm)	Surface area	d ₁₀₀ (nm) Surface area Pore Diameter	Wall thickness	Pore Volume
		$(m^2/g)^a$	_q (mu)	رسu)	_ρ (6/ _ε ωο)
MSU-X'	5.8	858	4.3	1.9	0.98
5% MP-MSU-X'	2.7	1079	3.7	2.2	1.04
10% MP-MSU-X'	2.7	1118	3.5	2.4	1.02
15% MP-MSU-X'	5.8	1021	3.0	3.0	0.82
20% MP-MSU-X'	5.0	936	2.9	2.4	0.72
25% MP-MSU-X'	6.2	775	2.5	3.4	0.53

model. c Wall thickness determined from the difference between d_{100} and pore diameter. d Pore volume determined at P/Po = 0.98 ^a Calculated by the Brunaeur-Emmett-Teller (BET) method. ^b Determined by the Horvath-Kawazoe

Table 2.5 29 Si NMR Cross-linking parameters for MP-MSU-X' assembled using Brij 56 surfactant

Material	Хехф	X _{cal}	Q⁴	Q ³	Q ²	Q ⁴ /Q ³ +Q ²	T ³	T²	$Q^4+T^3/$ Q^3+Q^2 $+T^2$	mmol SH/g
MSU-X'	-		0.68	0.30	0.03	2.06	-	-	2.06	-
MP-MSU-X'	0.15	0.13	0.52	0.32	0.04	1.45	0.10	0.02	1.63	2.3
MP-MSU-X'	0.20	0.16	0.52	0.30	0.04	1.53	0.10	0.04	1.65	2.5

²⁹Si MAS NMR of MP-MSU-X' (Brij 56)

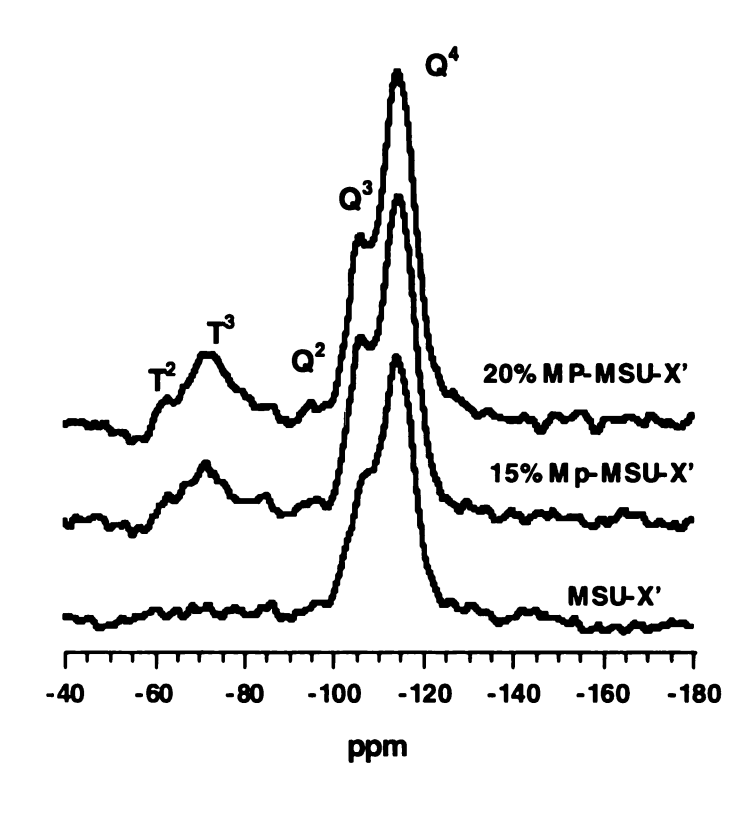


Figure 2.12 ²⁹Si MAS NMR spectra of MP-MSU-X' assembled using Brij 56 surfactant with different moles of MP

2.4 Conclusions:

The research objective was to functionalize silica mesostructures with wormhole framework structure in a one step synthesis procedure using costeffective sodium silicate reagents. This is the first example where a mesostructured material was assembled from sodium silicate as the silica source through a one step direct assembly procedure. Table 2.5 compares the properties of MP- MSU-X materials assembled using non-ionic surfactants and TEOS as the silica source and MP-MSU-X' derivative assembled in this work using water-soluble sodium silicate as the silica source. The modified assembly procedure based on sodium silicate resulted in the incorporation of up to 25 mole percent of the organosilane, as opposed to previously reported data for MP-MSU-X by Richer and Mercier²³ where the highest reported value was 5 mole percent. The sequence in which the reagents are combined probably plays a the major role in determining the percentage of organosilane that is incorporated in the material. In the present work the organosilane (MP) and the silica source (sodium silicate) are immiscible. To achieve miscibility, the organosilane is added first to the acidified surfactant acid solution and allowed to equilibrate for one hour. This results in the penetration of the organosilane into the hydrophobic core of the surfactant micelle. The organosilane reagent in this case then acts as a pore expander in the initial stages of assembly and a source of MP silane at later stages of assembly. This results in the incorporation of more MP groups into the framework walls during assembly. In the case of mesostructures assembled from TEOS the MP silane and TEOS are added simultaneously and

both reagents dissolve into the hydrophobic core of the surfactant micelle prior to assembly. The amount of MP incorporated into the framework under these conditions is then decided by the partitioning of the organosilane and TEOS between the micelle core and micelle surface where the mesostructure is formed.

	<u> </u>	
		3
		•
,		

Figure 2.13 Schematic representation of the steps involved in the assembly of MP-MSU-X' mesostructures from 3-mercaptoporopyltrimethoxysilane (3-MPTMS) and sodium silicate in the presence of Brij 56 surfactant. The electrical charge on the silicate anion and the bonding of Na⁺ to the PEO head groups are not shown for clarity.

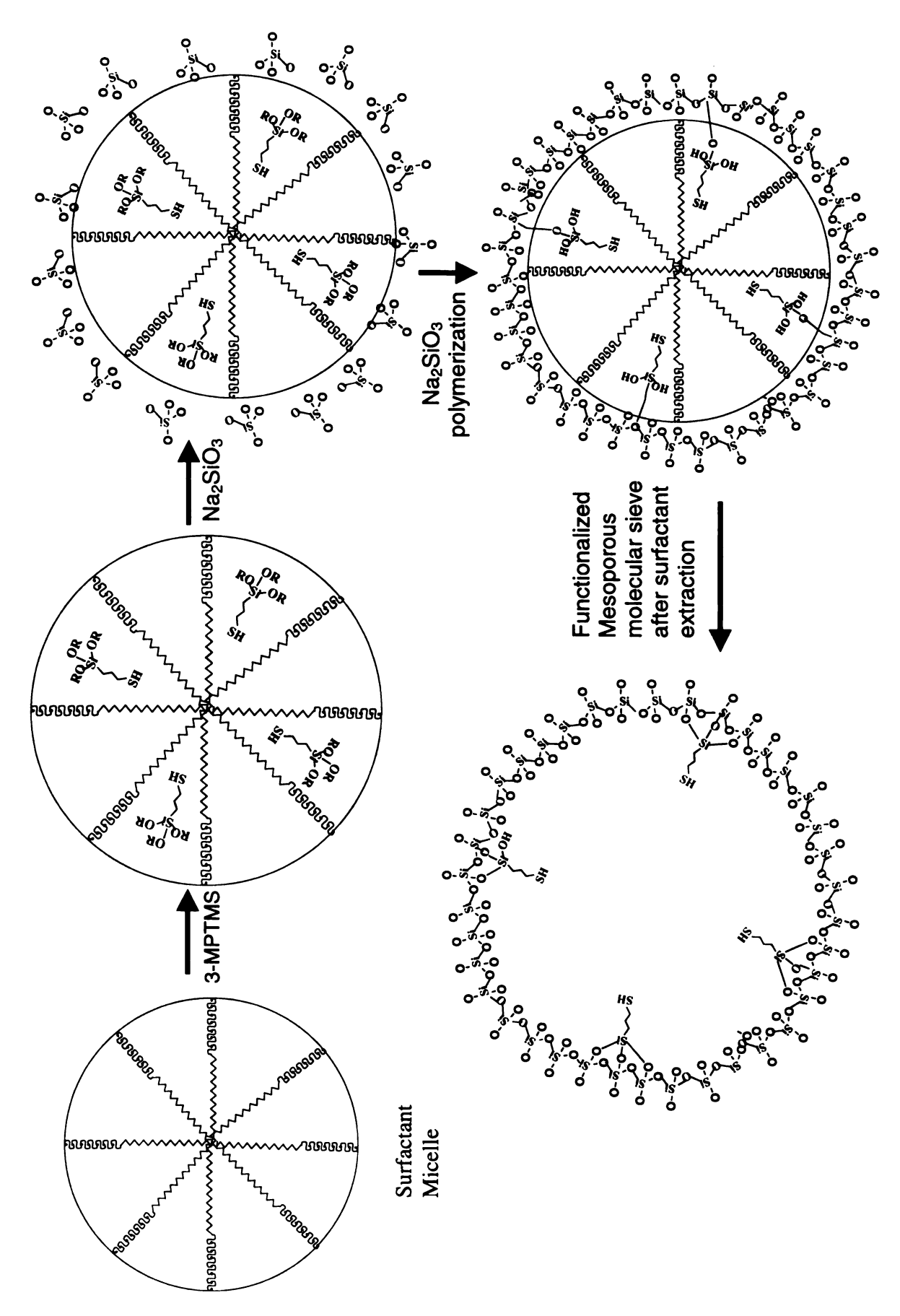


Table 2.6 Comparison of MP-MSU-X and MP-MSU-X' mesostructured materials assembled using various non-ionic surfactants

Material	Surfactant	Silica	Mol	d ₁₀₀	S.A.	Pore	Wall	Pore
		source	%	(nm)	m²/g	Size	Th.	Volume
			MPb			(nm)	(nm)	(cm ³ /g)
MSU-1 ²³	Brij-76	TEOS	0	7.9	630	6.9	1.0	0.53
MP-MSU-1 ²³	Brij-76	TEOS	2	7.9	1212	5.7	2.2	1.19
MP-MSU-1 ²³	Brij-76	TEOS	5	8.1	812	4.9	3.2	0.76
MSU-2 ²³	Triton-X100	TEOS	0	6.6	1018	4.1	2.5	
MP-MSU-2 ²³	Triton-X100	TEOS	2	6.3	1140	4.2	2.1	
MP-MSU-2 ²³	Triton-X100	TEOS	5	4.9	739	2.8	2.1	
MSU-X' ^a	Tween 80	Na ₂ SiO ₃	0	6.7	900	5.0	1.7	1.04
MP-MSU-X' ^a	Tween 80	Na₂SiO₃	5	6.7	829	4.4	2.3	0.74
MP-MSU-X' ^a	Tween 80	Na ₂ SiO ₃	15	6.9	490	3.6	3.3	0.42
MP-MSU-X' ^a	Tween 80	Na ₂ SiO ₃	25	7.1	163	2.5	4.1	0.11
MSU-X' ^a	Brij 56	Na ₂ SiO ₃	0	5.8	858	4.3	1.9	0.98
MP-MSU-X' ^a	Brij 56	Na ₂ SiO ₃	5	5.7	1079	3.7	2.2	1.04
MP-MSU-X'ª	Brij 56	Na ₂ SiO ₃	15	5.8	1021	3.0	3.0	0.82
MP-MSU-X' ^a	Brij 56	Na ₂ SiO ₃	25	6.2	775	2.5	3.4	0.53

^a Present work ^b 3-Mercaptopropyltrimethoxysilane

Results discussed herein, together with those presented previously by Zhang and Pinnavaia, Bagshaw^{18,21,24} and Prouzet et al^{18,20,21,24-26} lead to the conclusion that cations exert structure-directing effects on a proposed flexible PEO/M⁺/silicate complex and leads to modified pore symmetries over materials formed in neutral solutions. This result is also evident from the X-ray patterns for the MP-MSU-X' derivative containing higher levels of organofunctionalization. As the amount of organosilane reagent increases the amount of sodium silicate added to the reaction mixture decreases reducing the number of sodium ions in the system. This leads to the formation of a purely wormhole structure rather than a hexagonal structure. Thus, an accurate descriptor for the assembly mechanism would be N⁰M⁺X⁻I⁰ where M⁺ is the cation and X⁻ is the counter anion; acetate anion in the present case.

2.5 References:

- (1) Beck, J. S., Vartuli, J.C., Roth, W.J., Leonowicz, M.E., Kresge, C.T., Schmitt, K.D., Chu, C.T-W., Olson, D.H., Sheppard, E.W., McCullen, B., Higgins, J.B., Schlenker, J.L. *Journal of American Chemical Society* **1992**, *114*, 10834.
 - (2) Q.Huo, R. L., P.M.Petroff, G.D.Stucky Science 1995, 268, 1324.
- (3) Q.Huo, D. I. M., U.Ciesla, P. Feng, T.E. Gier, P.Sieger, R.Leon, P.M.Petroff, F. Schuth, G.D.Stucky *Nature* **1994**, *368*, 317.
 - (4) Tanev, P. T.; Pinnavaia, T. J. Science 1995, 267, 865-867.
- (5) Bagshaw, S. A.; Prouzet, E.; Pinnavaia, T. J. *Science* **1995**, *269*, 1242-1244.
- (6) Bagshaw, S. A.; Pinnavaia, T. J. *Angew. Chem.-Int. Edit. Engl.* **1996**, *35*, 1102-1105.
- (7) Prouzet, E.; Pinnavaia, T. J. *Angew. Chem.-Int. Edit. Engl.* **1997**, *36*, 516-518.
- (8) Antonelli, D. M.; Ying, J. Y. *Angew. Chem.-Int. Edit. Engl.* **1996**, *35*, 426-430.
 - (9) Antonelli, D. M.; Ying, J. Y. Chem. Mat. 1996, 8, 874-881.
 - (10) L.Sierra, B. L., J.Gil and J-L Guth Adv. Mater. 1999, 11, 307.
 - (11) L.Sierra, a. J.-L. G. Microporous Mesoporous Mat. 1999, 27, 243.
 - (12) S-S. Kim, T. R. P., T.J.Pinnavaia *Chem. Commun.* **2000**, *835*.
 - (13) S-S. Kim, T. R. P., T.J.Pinnavaia Chem. Commun. 2000, 1661.

- (14) Sing, K. S. W.; Everett, D. H.; Haul, R. A. W.; Moscou, L.; Pierotti, R. A.; Rouquerol, J.; Siemieniewska, T. *Pure Appl. Chem.* **1985**, *57*, 603-619.
 - (15) Horvath, G.; Kawazoe, K. J. Chem. Eng. Jpn. 1983, 16, 470-475.
 - (16) Porter, M. R. Handbook of Surfactants, 1994.
- (17) Brinker, C. J. a. S., G. W. Sol-Gel Science: The Physiscs and Chemistry of Sol-Gel Processing; Academic Press: San Diego, 1990.
 - (18) Bagshaw, S. A. Chem. Commun. 1999, 1785-1786.
- (19) Zhang, W. Z. G., B.; Pauly, T.; Pinnavaia, TJ *Chem. Commun.* **1999**, 1803-1804.
- (20) Prouzet, E.; Cot, F.; Nabias, G.; Larbot, A.; Kooyman, P.; Pinnavaia, T. J. *Chem. Mat.* **1999**, *11*, 1498-1503.
 - (21) Bagshaw, S. A. J. Mater. Chem. 2001, 11, 831-840.
- (22) Siew D.C.W, C. R. P., Taylor M.J., Easteal a.J. *J. Chem. Soc.,* Faeaday Trans. **1990**, *86*, 1109.
 - (23) Richer, R. M., L. Chem. Mat. 2001, 13, 2999-3008.
 - (24) Bagshaw, S. A. Chem. Commun. 1999, 271-272.
- (25) Boissiere, C.; Larbot, A.; Prouzet, E. *Chem. Mat.* **2000**, *12*, 1937-1940.
- (26) Boissiere, C.; Larbot, A.; van der Lee, A.; Kooyman, P. J.; Prouzet, E. *Chem. Mat.* **2000**, *12*, 2902-2913.

Chapter 3

Future Goals

3.1 Functionalization of MSU-X' mesostructures with other organosilanes:

The work presented here accomplished the organofunctionalization of mesostructures assembled from organosilane reagents and cost effective watersoluble silicates in the presence of non-toxic, biodegradable PEO surfactant. The organosilane chosen was 3-Mercaptopropyltrimethoxysilane. mesostructures so functionalized should find use as heavy metal ion traps, especially for mercury trapping and as a precursor to heterogeneous acid catalysts. The materials were characterized by PXRD, N₂ adsorption-desorption isotherms, ²⁹Si NMR and TEM. The functionalized mesostructures are comparable to grafted FMMS (Functionalized Mesoporous Molecular Sieve)¹ mesostructures in the fidelity of the pore structure and the surface area properties. The cross linking for these materials is greatly improved offering possibility of improved hydrolytic stability.

Future work will determine the general usefulness of the assembly pathway with regard to other organosilane reagents. The model depicted in Figure 2.13 partitions the organosilane at the lipophilic region of the surfactant micelle and serves as a reservoir for the transfer of the organosilane to the framework being assembled at the micelle solution interface.

The model will be further tested with other organophilic organosilane reagents for its general applicability. Organosilanes containing alkyl, phenyl,

nitriles, halides etc. will be tested. Functionalization with amine terminated mono (3-aminopropylsilane) and diamines (ethylenediamine) will be interesting as these silanes are more polar in nature.

3.2 Functionalization of large pore foam like MSU-F mesostructures:

Molecular sieves with uniform and well-defined pores are promising materials for a variety of applications in catalysis, separation, ion exchange and sensory materials. Amphiphilic block copolymers have turned out to be valuable supramolecular templates for creating mesostructured materials possessing long-range order. Aside from employing different kinds of surfactants,^{2,3} the assembly mesoporous materials has been controlled by changing the hydrophobic volumes of the templates, which can be achieved by changing the reaction temperature or by adding organic co -solvents as swelling agents.⁴⁻⁶

Recently well-defined macroporous and large-pore mesoporous materials have been assembled using either emulsions⁴⁻⁸ or polymer latex spheres as templates.^{9,10} However, these materials are tedious and time consuming to prepare. Stucky and coworkers¹¹ have used microemulsions as colloidal templates for the synthesis of Mesostructured Cellular Foams (MCF). The MCFs are assembled at acidic pH from oil in water microemulsions from triblock copolymer surfactant (EO₂₀ PO₇₀ EO₂₀) P123, 1,3,5-Trimethylbenzene (TMB) as the organic swelling agent and TEOS as the silica source. Stucky and coworkers were able to tailor the pore sixes in the range of 10-100 nm.

Pinnavaia and coworkers¹² used cost effective reagents to assemble MSU-F materials, which are comparable to MCF materials. MSU-F materials are also

assembled via microemulsion templating route but the synthesis is carried out at near neutral pH conditions and cost effective sodium silicate as the silica source.

The direct one-step assembly of organofunctionalized large pore MSU-F materials could be very attractive for their use in various applications in catalysis, ion exchange, and separation. The pore sizes for these materials can be tailored from 10-100 nm. Since the materials have very large pore diameters it could be expected that one could introduce larger amount of functional group into the material before the pores get blocked and the material becomes microporous. In the organofunctional wormhole structure prepared in the present work, only 25% of the framework silicon centers were organofuctionalized before the pores became blocked. Much large loadings should be possible for MSU-F mesostructures.

Functionalization of mesoporous materials by direct assembly process requires that there is no phase separation between the reagents used. This was a challenge for the synthesis of mesostructures assembled from water-soluble silica sources, which was overcome by using concentrated acids and modifying the sequence in which the reagents were added. Functionalization of MSU-F mesostructures poses another problem. The mesostructure is assembled via oil in water microemulsion as the template around which the silica condenses. The alkoxides are moisture sensitive and to facilitate formation of emulsions the water phase need to be replaced with some other polar solvent. Many apolar liquids can be emulsified in formamide using triblock copolymers of ethylene oxide and propylene oxide as the surfactant. The droplet phase can be any apolar liquid

used in the more conventional aqueous medium. Imhof and Pine¹³ have used non-aqueous emulsions for the preparation of titania foams from titanium tetraisopropoxide a water sensitive reagent.

The use of non-aqueous solvents in the functionalization of large pore MSU-F materials will be explored in future work.

3.3 Functionalization of MSU-SA mesostructures:

Mesoporous HMS silicas with small, intergrown domains and sponge like particle textures are synthesized using long alkyl chain amines as the structure directing surfactant and TEOS as the silica source. Recently Pinnavaia and coworkers¹⁴ have achieved up to 50% functionalization of HMS mesostructures. The sponge like particle texture improves the framework asseccibility. Presently, these materials are made from costly molecular silica precursors such as TEOS.

MSU-SA¹⁵ mesostructures, which are analogs of HMS mesostructures, are assembled using neutral amine surfactants and water-soluble sodium silicate. These materials exhibit similar physical properties as HMS materials and depict the same wormhole framework morphology and a high textural porosity. The one-step direct functionalization of MSU-SA materials has several advantages. The combined use of inexpensive primary amine or commercially available polyamines along with cost effective water—soluble silicate sources should offer an efficient low cost route to functionalized mesostructured silicas.

3.4 References:

- (1) Feng, X.; Fryxell, G. E.; Wang, L. Q.; Kim, A. Y.; Liu, J.; Kemner, K. M. *Science* **1997**, *276*, 923-926.
- (2) Ying, J. Y.; Mehnert, C. P.; Wong, M. S. *Angew. Chem.-Int. Edit.* **1999**, *38*, 56-77.
- (3) Ciesla, U.; Schuth, F. *Microporous Mesoporous Mat.* 1999, 27, 131-149.
- (4) D.Zhao, J. F., Q. Hou, B.F.Chmelka, G.D.Stucky *Journal of American Chemical Society* **1998**, *120*, 6024.
- (5) D.Zhao, J. F., Q. Hou, N.Melosh, G.H.Fredrickson, B.F.Chmelka, G.D.Stucky *Science* **1998**, *279*, 548.
- (6) Prouzet, E.; Pinnavaia, T. J. *Angew. Chem.-Int. Edit. Engl.* **1997**, *36*, 516-518.
- (7) Imhof, A.; Pine, D. J. J. Colloid Interface Sci. 1997, 192, 368-374.
- (8) Imhof, A.; Pine, D. J. Chem. Eng. Technol. 1998, 21, 682-685.
- (9) Holland, B. T.; Blanford, C. F.; Stein, A. *Science* **1998**, *281*, 538-540.
- (10) Holland, B. T.; Blanford, C. F.; Do, T.; Stein, A. Chem. Mat. 1999, 11, 795-805.
- (11) Schmidt-Winkel, P.; Lukens, W. W.; Yang, P. D.; Margolese, D. I.; Lettow,J. S.; Ying, J. Y.; Stucky, G. D. *Chem. Mat.* 2000, *12*, 686-696.
- (12) S-S. Kim, T. R. P., T.J.Pinnavaia Chem. Commun. 2000, 1661.
- (13) Imhof, A.; Pine, D. J. Adv. Mater. 1999, 11, 311-314.
- (14) Mori, Y.; Pinnavaia, T. J. Chem. Mat. 2001, 13, 2173-2178.

(15) Pauly, T. R. In *Chemistry*; Michigan State University: East Lansing, 2000, pp 180-217.

